



Field Trip Guide Book - B17

Florence - Italy
August 20-28, 2004

Volume n° 2 - from B16 to B33

**32nd INTERNATIONAL
GEOLOGICAL CONGRESS**

**THE PERIADRIATIC
INTRUSION OF VEDRETTE
DI RIES - RIESERFERNER
(EASTERN ALPS):
PETROLOGY,
EMPLACEMENT MECHANISMS
AND CONTACT AUREOLE**



Leaders: B. Cesare, A.M. Fioretti, C. Rosenberg

Pre-Congress

B17

The scientific content of this guide is under the total responsibility of the Authors

Published by:

**APAT – Italian Agency for the Environmental Protection and Technical Services - Via Vitaliano
Brancati, 48 - 00144 Roma - Italy**



Series Editors:

Luca Guerrieri, Irene Rischia and Leonello Serva (APAT, Roma)

English Desk-copy Editors:

**Paul Mazza (Università di Firenze), Jessica Ann Thonn (Università di Firenze), Nathalie Marlène
Adams (Università di Firenze), Miriam Friedman (Università di Firenze), Kate Eadie (Freelance
independent professional)**

Field Trip Committee:

**Leonello Serva (APAT, Roma), Alessandro Michetti (Università dell'Insubria, Como), Giulio Pavia
(Università di Torino), Raffaele Pignone (Servizio Geologico Regione Emilia-Romagna, Bologna) and
Riccardo Polino (CNR, Torino)**

Acknowledgments:

**The 32nd IGC Organizing Committee is grateful to Roberto Pompili and Elisa Brustia (APAT, Roma)
for their collaboration in editing.**

Graphic project:

Full snc - Firenze

Layout and press:

Lito Terrazzi srl - Firenze

Volume n° 2 - from B16 to B33



**32nd INTERNATIONAL
GEOLOGICAL CONGRESS**

**THE PERIADRIATIC INTRUSION
OF VEDRETTE DI RIES - RIESERFERNER
(EASTERN ALPS): PETROLOGY,
EMPLACEMENT MECHANISMS
AND CONTACT AUREOLE**

AUTHORS:

B. Cesare^{1,2}, A.M. Fioretti², C. Rosenberg³

¹Dipartimento di Mineralogia e Petrologia, Università di Padova - Italy

²C.N.R. Istituto di Geoscienze e Georisorse, Sezione di Padova - Italy

³Department of Geology, Freie Universität, Berlin - Germany

**Florence - Italy
August 20-28, 2004**

Pre-Congress

B17

Front Cover:

*The Collalto - Hochgall (3436 m a.s.l.)
is the highest peak of the Vedrette di Ries massif.
It is composed of fine-grained tonalite.*

Leaders: B. Cesare, A.M. Fioretti, C. Rosenberg

Introduction

During the Oligocene the Alpine chain was the centre of an extensive magmatism, mainly represented by calc-alkaline, which resulted in a series of plutons situated along and adjacent to the Periadriatic Lineament. These intrusives are hence referred to as "Periadriatic plutons".

With an outcrop length of approximately 40 km, and a vertical exposure of 2500 m from base to roof, Vedrette di Ries (Rieserferner) represents one of the best exposed plutons worldwide (Figure 1).

The intrusion of the pluton is characterised by three major pulses of tonalitic to granodioritic composition, with distinct petrographic and geochemical signatures. The ascent of these magmas was controlled by the Deferegggen-Anterselva-Valles (DAV) line, which strikes along large parts of the southern margin of the pluton. The contact aureole of the intrusion developed in the metapelitic country rocks, and is characterised by a complete zoneography from andalusite-staurolite to sillimanite-K-feldspar. The presence of synmetamorphic andalusite-bearing veins, related to the dehydration of metapelites, is a unique feature of

this contact aureole.

During the field trip we will show the key outcrops of the pluton, discussing both the results and the new ideas arising from detailed structural, petrologic and geochemical investigations performed over the past twenty years.

Geologic and topographic maps

1:25.000 topographic map, sheet n. 035 "Valle Aurina - Vedrette di Ries", Ed. Tabacco.

Cammelli F. (1994) Alpi pusteresi. Guida escursionistico-alpinistica. Available also in German, Ed. Athesia.

Carta Geologica d'Italia 1:100.000, sheet n. 4b "Dobbiaco".

Geologic Map of Italy 1:50.000, sheet n. 009 "Anterselva" (in print).

Hammerschmidt K. 1981 Isotopengeologische Untersuchungen am Augengneis vom Typ Campo Tures bei Rain in Taufers, Südtirol. Mem.Sci.Geol., 34, 273-300, with geologic map.

Mager D. 1985 Geologische Karte des Rieserfernergruppe zwischen Magerstein und Windschar (Südtirol). 'Der Schlern', 6, Bozen.



Figure 1 - Geologic map of the Eastern Alto Adige (South Tyrol) from Dal Piaz (1934)

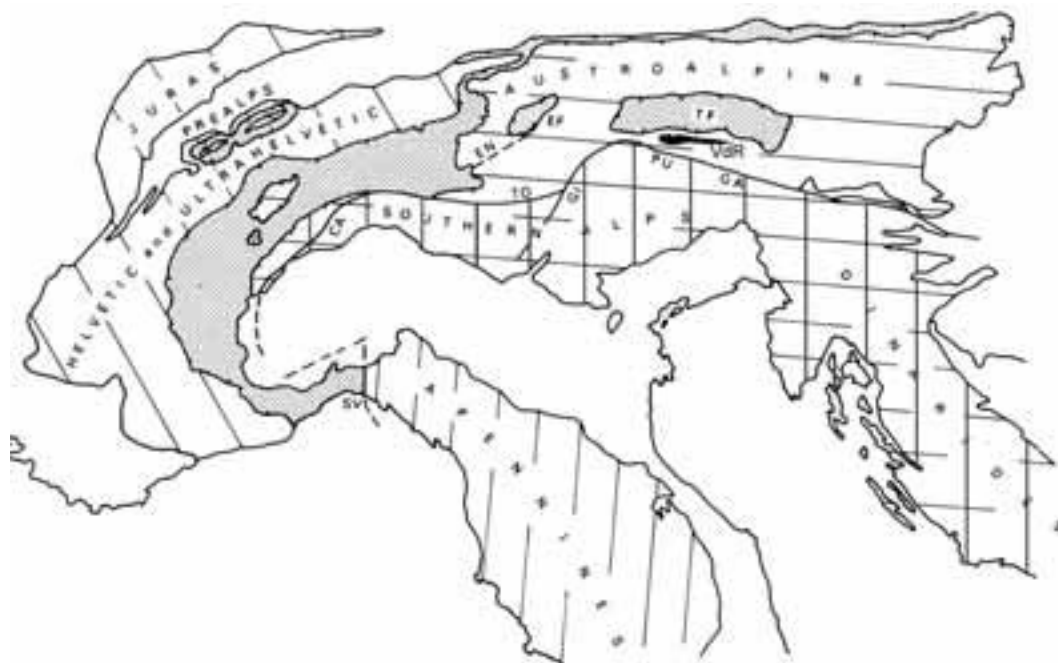


Figure 2 - Main Structural and paleogeographical domains of the Alps (from Dal Piaz et al., 1975).

Schulz B. (1994) Geologische Karte des Altkristallin östlich des Tauferer Tals. Erlanger Geol. Abh., 124; 1-28.

Senarclens-Grancy W. (1972) Geologische Karte der westlichen Deferegger Alpen, Ostirol, 1:25.000. Geol. B. A., Wien.

Regional geologic setting

The Alpine chain (Figure 2) may be subdivided into the following paleogeographic domains (e.g. Froitheim et al., 1996): (1) The European margin, represented by the Helvetic cover nappes, the external massifs, and the lowermost penninic nappes; (2) the Adriatic (Apulian and Insubric) margin, found in the Austroalpine basement and cover nappes north of the Periadriatic Line and by the unmetamorphosed Southalpine nappes south of the Periadriatic Line; (3) the remnants of two oceanic domains (the Valais ocean and the Piedmont-Ligurian ocean), represented by ophiolites and «Buendnerschiefer», located along the contact between the European and Adriatic units; (4) the Briançonnais, a microcontinent separating the two oceanic domains, found in the uppermost Penninic Units and the cover nappes of the «Préalpes Romandes» in Switzerland.

Most of these units are outcropping in the area of the Vedrette di Ries pluton. The Dolomites, south

of the pluton, belong to the Southalpine domain; the Austroalpine basement makes the country rock of the intrusion. The latter unit(=the basement? the Briançonnais?) are thrust over the oceanic and European units, as can be seen in a large tectonic window (the Tauern window) north of Vedrette di Ries. The oceanic units form the border of the Tauern window (Schieferhuelle), whilst its core exposes basement rocks (Zentral Gneiss) from the European margin.

Eclogites of Cretaceous as well as Tertiary age occur in the Alps. The former ones are found in the Austroalpine domains, whereas the latter ones are part of the Penninic and ophiolitic units of the Valais and Piedmont-Ligurian oceans. These two ages of eclogitization correspond to different tectonic events which occurred in different parts of the Alpine region (Froitheim et al., 1996). Cretaceous eclogite metamorphism results from the closure of the Meliata-Halstatt ocean (Neubauer, 1994), a Triassic ocean whose remnants are found from the Carpathians to the eastern Alps (Kozur, 1991). In contrast, Tertiary eclogites reflect the subduction of the Jurassic Piedmont-Ligurian ocean (early Paleocene), followed by that of the Valais ocean (early Eocene), below the Adriatic plate. Parts of the European continental margin were also subducted, as

shown by the occurrence of high-pressure and ultra-high pressure rocks in the Dora Maira massif of the western Alps (Chopin et al., 1991).

During the Oligo-Miocene the eastern Alps and the area of Vedrette di Ries were affected by intense N-S shortening, contemporaneous with orogen-parallel extension, resulting in eastward extrusion. This tectonic regime formed large pop-up structures (the Tauern Window), delimited by syn-convergence, low angle normal faults at its eastern (the Brenner Fault) and western margins (the Katschberg Fault). Lateral extrusion, was accommodated by sets of conjugate dextral (e.g., the Periadriatic Line) and sinistral (e.g., the SEMP Line) strike-slip faults. The widespread occurrence of subhorizontal E-W striking stretching lineations and fold axes in the country rocks of Vedrette di Ries records this phase of orogen-parallel extension.

Ongoing shortening and thickening of the orogen caused a propagation of the deformation front towards the more external zones of the chain in the middle- to late Miocene. Hence, the Jura Mountains and thrusting in the Molasse basin were initiated to the north of the Alps, whilst thrusting in the Southern

Alps and in the Po Plain affected the southern part of the chain.

The Periadriatic Magmatism and Vedrette di Ries.

The Periadriatic magmatism took place along the entire Alpine chain during the Oligocene, (Exner, 1976; Laubscher, 1985) i.e., long after the continental collision between the African (Insubric) and European plates, which occurred starting from the Eocene. Based on their andesitic, calc-alkaline characters and geological setting these magmas were interpreted as products of a subduction process (Sassi et al., 1980, Bellieni et al., 1981, Kagami, 1991). Dal Piaz & Venturelli (1983) and Laubscher (1985) questioned this interpretation, and proposed that the magmatism, postdating the main tectono-metamorphic event related to the collision, developed during a short extensional phase following the continental collision. According to these authors this extensional phase triggered the ascent and emplacement of the Periadriatic plutons along a belt extending for ca. 700 km from the western Traversella body, in the Piemonte region, to the eastern Pohorje pluton in

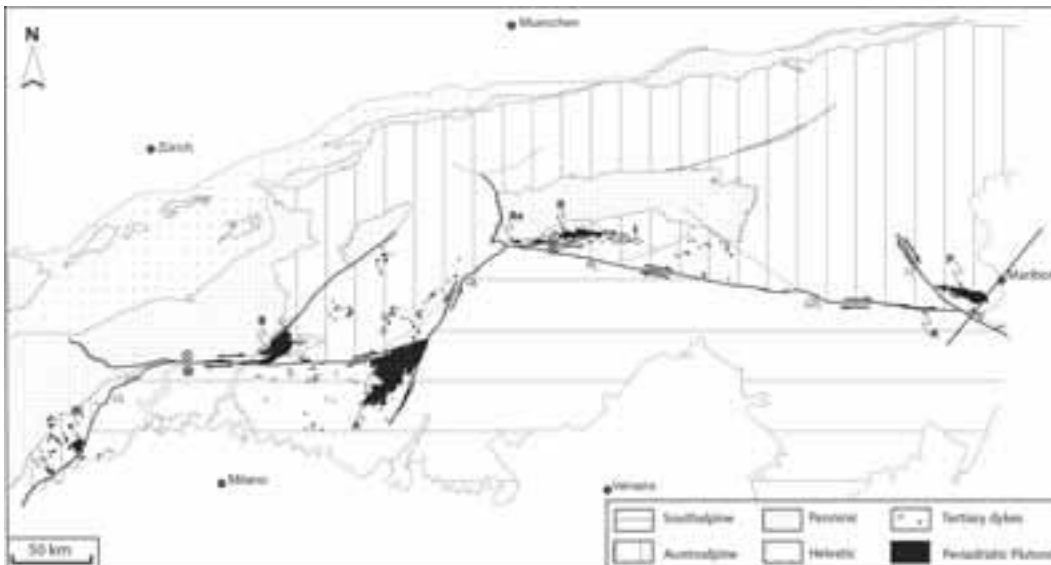


Figure 3 - Simplified tectonic map of the Alps, with enlargements of some segments of the PFS showing the spatial distribution of the Oligo-Miocene dikes and of the Periadriatic plutons. Only the major faults of Tertiary age are shown. Redrawn after Bigi et al. (1990). Faults: CL: Canavese Line; DAV: DAV Line; GL: Giudicarie Line; GTL: Gailtal Line; IL: Insubric Line; LT: Lavantal Line; PL: Pustertal Line. Plutons: A: Adamello; An: Andesites of the Canavese Line; B: Bergell; Bi: Biella; K: Karawanken; L: Lesachtal body; M: Miagliano pluton; P: Pohorje; R: Rieserferner; Re: Rensen; T: Traversella; TL: Tonalitic Lamellae. Full circles: dikes.

Note that only part of the dikes are dated. Most of them are inferred to be Oligocene on the basis both of petrographic analogy with the dated ones and of crosscutting relationships with their country rocks.

The size of the dikes is exaggerated by several orders of magnitude.

Slovenia (Figure 3).

However, structural investigations of some of these plutons showed that ascent and emplacement occurred in a transpressive tectonic setting (Rosenberg et al., 1995; Steenken, 2000; Rosenberg, in press). The latter interpretation is consistent with the generation of the Periadriatic magmas by slab break-off, as suggested by the distribution of the magmatic bodies and their geochemical signature (Von Blanckenburg and Davis, 1995).

The Periadriatic magmatism includes plutonic and volcanic rocks of calc-alkaline orogenic series, as well as dikes ranging from andesitic to shoshonitic and ultrapotassic lamprophiric compositions. The whole Periadriatic magmatism can be subdivided into three main sectors. In the western sector, with a NE-SW orientation, plutons intrude mainly the Southern Alps and extend up to the limit with the overthrust Austroalpine continental crust. Magmatism is represented by small plutons, volcanic covers and high-K andesitic dikes (Dal Piaz and Venturelli, 1983). In the central sector the Periadriatic magmatism reaches its widest extension and is represented by the Adamello batholith, which intruded the South Alpine basement and its Permo-Mesozoic sedimentary cover, and by the Bregaglia-Iorio pluton intruding five nappes of the Alpine pile, including Penninic crystalline, ophiolites and Austroalpine crust (Trommsdorff and Nievergelt, 1983).

In the eastern Alps the Periadriatic magmatism is concentrated in the Austroalpine domain. Only minor occurrences are reported in the northern part of the Southern Alps (Dal Piaz and Venturelli, 1983). In this sector of the chain most plutons (Rensen, Monte Alto –Altberg, Cima di Vila – Zinsnock, Vedrette di Ries) have an overall E-W elongated shape, reflecting their emplacement along the active Periadriatic lineaments. Vedrette di Ries constitutes the main plutonic body of the eastern Periadriatic magmatism. The smaller Cima di Vila pluton, once considered part of the Vedrette di Ries plutonic complex, is now recognized as a geochemically distinct magmatic body (Bellieni, 1980; Bellieni et al., 1982).

Geometry and emplacement of the pluton

Post-intrusive tilting of the pluton (Borsi et al., 1978; Steenken et al., 2002) and 2000 m of relief provide an exceptional exposure of the intrusive body, allowing us to reconstruct its 3D geometry (Figure 4). The roof of the pluton crops out over several tens of square kilometers in the central and northern

parts of the intrusion, and the base is exposed at its westernmost end. The main body of the pluton is ~2 km thick, relatively flat-lying and becomes steeply south-dipping, as it gets closer to the DAV (Figure 5). The contact between the fine-grained and the coarse-grained tonalites is subhorizontal in the gently-dipping main body of the pluton (Figure 5)

The foliation pattern in the main body of the intrusion (Figure 6) and a contour map of the contact (Figure 4) show that the roof of the pluton consists of two domal structures separated by a synform. The north-south striking axial plane of the synform is perpendicular to all regional structures of the country rocks away from the pluton, suggesting that this fold and the associated domes result from forceful emplacement of the tonalite rather than from regional deformation (Wagner et al., in review).

Large parts of the roof are discordant to the foliation in the country rocks, but there is no field evidence for stoping. Stopped blocks are lacking (Steenken et al., 2000) and rare xenoliths, generally < 50 cm long, only occur in the immediate vicinity of the contact. Hence, instead of stoping, the discordant contacts are inferred as resulting from extensional fracturing along a gently inclined plane (Figure 7; Wagner et al., in review).

The southern margin of the intrusion is steeply dipping to the south, parallel to the foliation of the country rocks and to the DAV (Figure 5). Locally preserved magmatic fabrics, oriented parallel to the solid-state mylonites of the DAV, suggest a syntectonic intrusion.

Within parts of this steep zone, concentric foliation patterns with steeply plunging magmatic lineations (Steenken et al. 2000; Wagner et al., in review) are found from the outcrop scale to that of several hundreds of meters (Figure 6). Such structures do not occur in other parts of the pluton, nor in the enclosing rocks.

The spatial coincidence of these structures with the steeply oriented part of the pluton suggests that this zone acted as the feeder for the intrusion (Figure 7). Therefore, ascent of the tonalitic magmas occurred in the southern part of the pluton, adjacent to the DAV mylonites. As a result of tilting, the easternmost continuation of the steep zone (the eastern tail of the pluton in map view) represents a higher crustal level than the main body and is therefore inferred as representing the upper continuation of the Vedrette feeder (Figure 7), which may have fed other plutons at higher crustal levels.

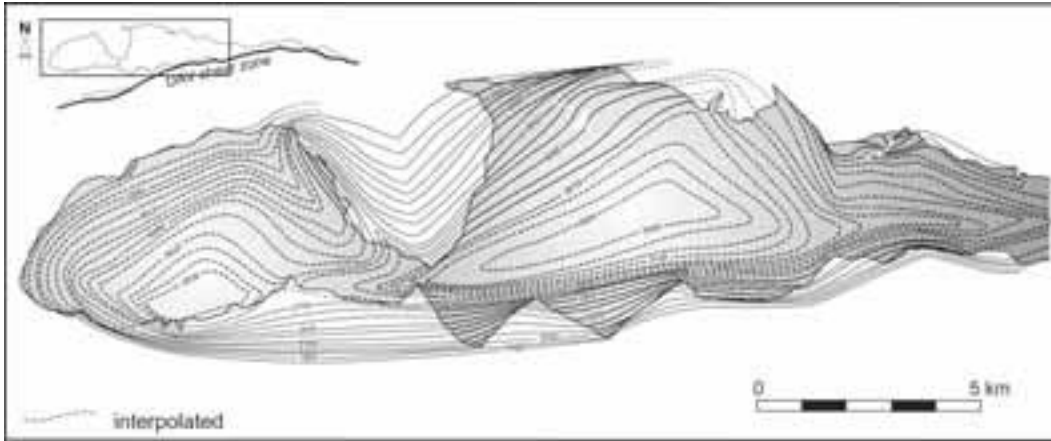


Figure 4 - Contour map of the pluton contact. Modified after Wagner et al., in review.

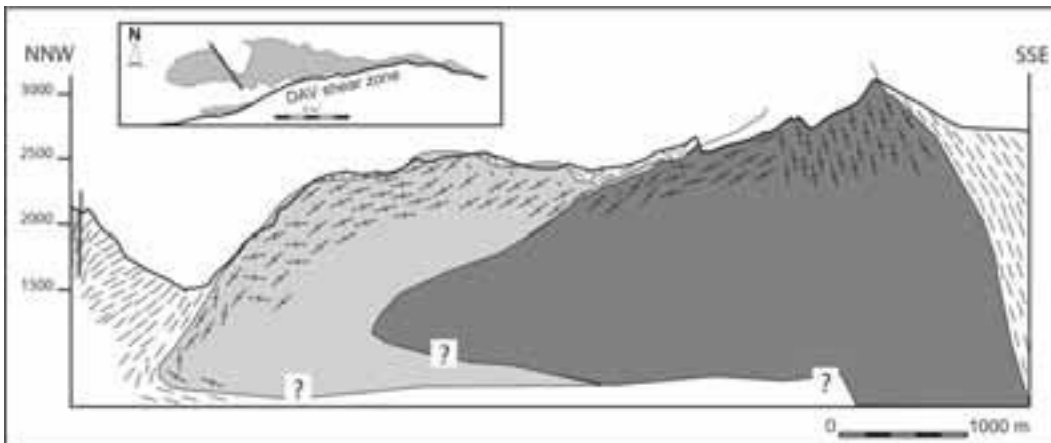


Figure 5 - N-S cross-section of the pluton. From Rosenberg, in press.

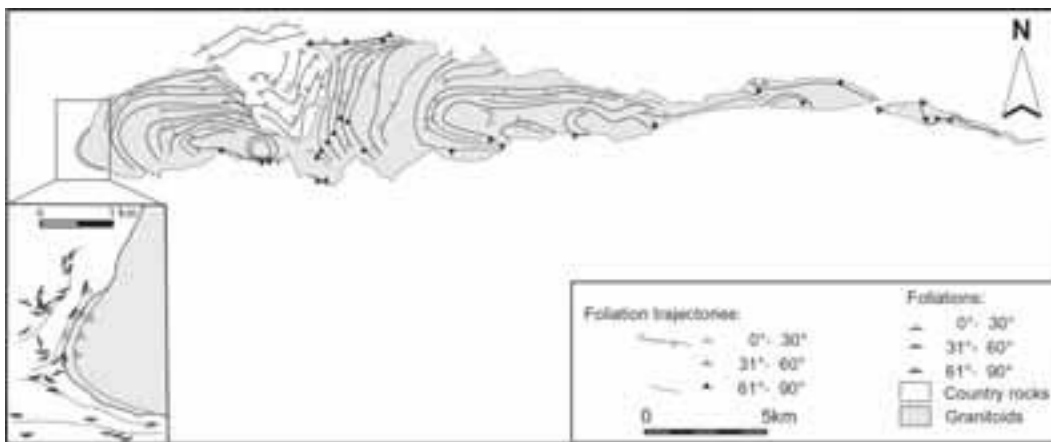


Figure 6 - Foliation trajectories in the Vedrette di Ries.

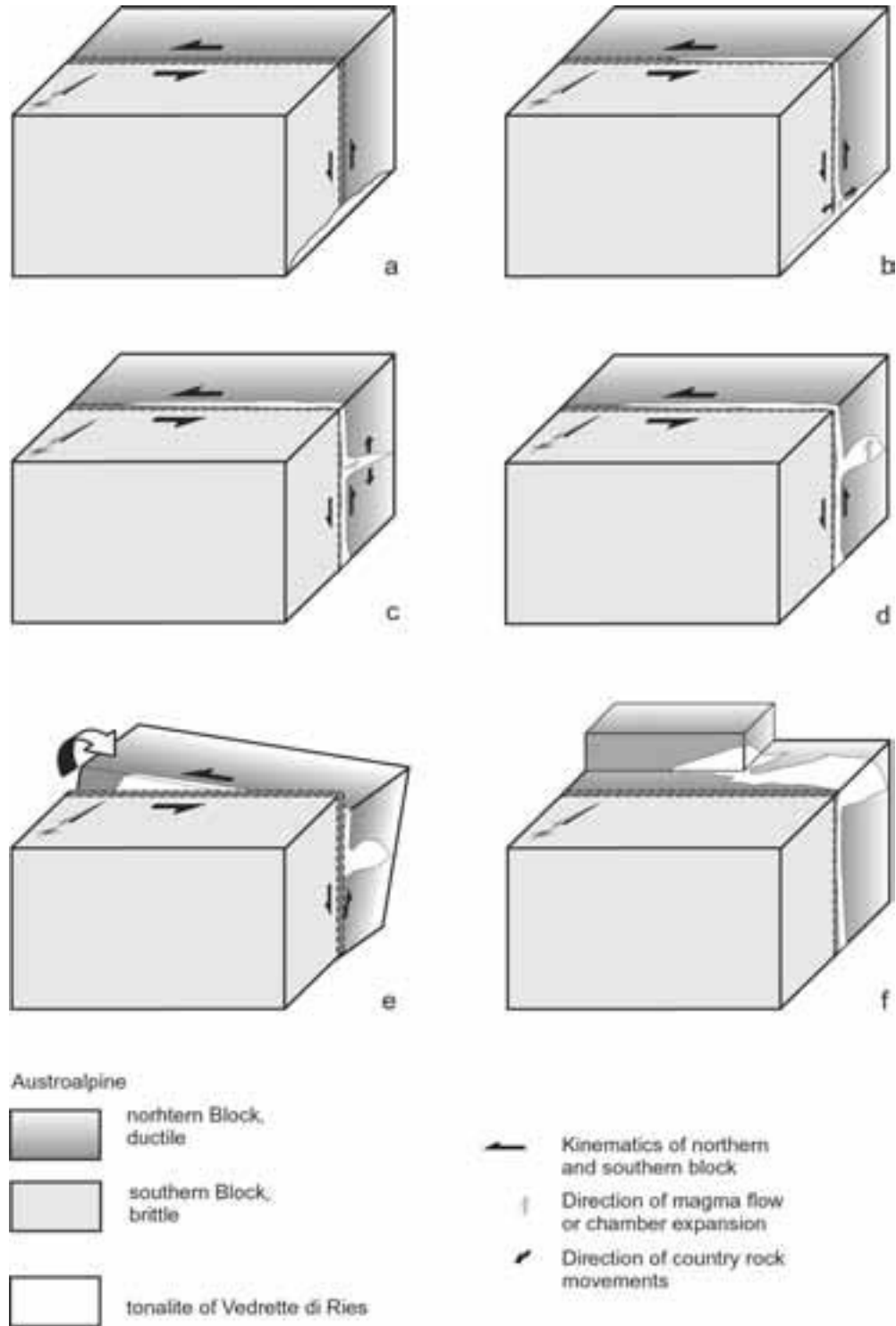


Figure 7 - Ascent and emplacement model for the Vedrette di Ries pluton, from Wagner et al., (2003).

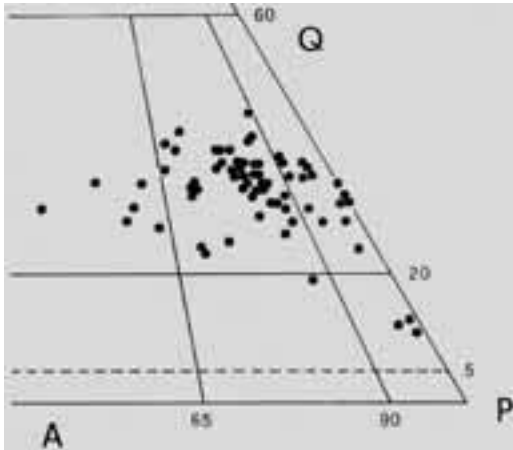


Figure 8 - Distribution of Vedrette di Ries rocks on the QAP classification diagram (taken from Bellieni et al., 1976).

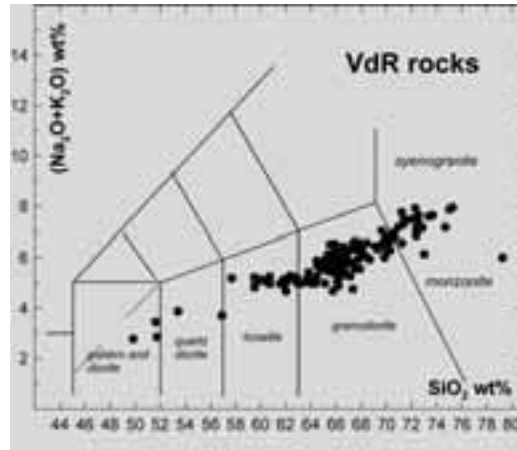


Figure 9 - TAS (Total Alkali Silica, Bellieni et al., 1995) classification diagram for rocks from the Vedrette di Ries pluton.

Igneous lithologies and field relationships.

Vedrette di Ries is a composite pluton, consisting mainly of granodiorite and tonalite, with minor amounts of granite and diorite (Figure 8 and Figure 9).

Three main suites of rocks can be distinguished both in the field and from their geochemical characteristics (Bellieni et al. 1976, Bellieni et al., 1981, Steenken et al., 2000).

Following their emplacement order we distinguish a **first, coarse-grained suite** (Figure 10), characterized by the presence of “book biotite” in piles up to 0.5 cm thick, stubby amphibole, and up to centimetric magmatic garnet (Bellieni et al., 1979, Bassani et al., 1997).

Rocks of this suite are mainly located in the western part of the body and discontinuously decorate its northern and, to a lesser extent, southern borders

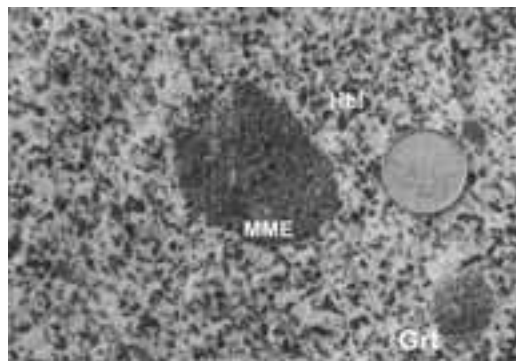


Figure 10 - Coarse-grained tonalite with up to centimetric garnet (Grt), stubby amphibole (Hbl), and frequent Mafic Microgranular Enclaves (MME)

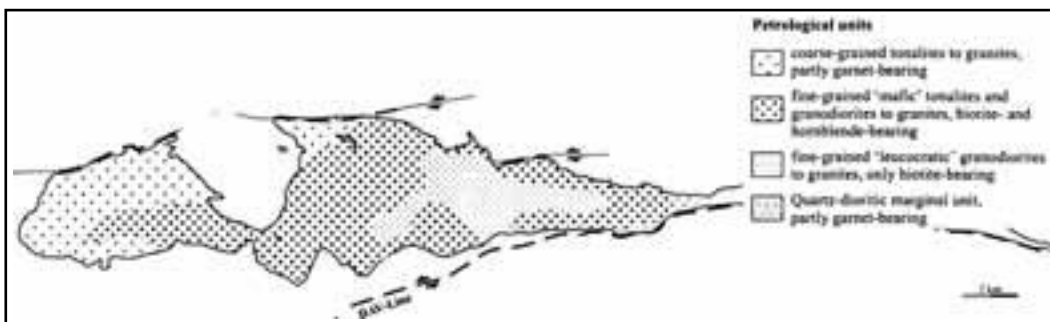


Figure 11 - Distribution of the various magmatic suites in the Vedrette di Ries Pluton (from Steenken et al. 2000).



Figure 12 - Sharp contact between coarse-grained garnet tonalite from suite 1 (right) and medium-grained granodiorite from suite 2 (left). Transitional contacts were observed in other places. As a rule, mafic microgranular enclaves are more abundant in tonalite than in granodiorite (2 km E of Ponte Tobel, a small quarry on the right side of the Reintal).

(Figure 11). This suite ranges in composition from diorite to granodiorite, with dominant tonalite. Small dioritic bodies are located along the south-eastern



Figure 13 - Initial stage of mingling between granodiorite and tonalite of the second, medium- to fine-grained suite (Western Gelta, area N of Rauchkofel, 2500m asl).

side of the pluton. Granite is rare and its affiliation to the suite is evidenced by the presence of rare garnet. The contacts among different lithologies are generally transitional with local evidence of mixing, although sharp contacts are also observed (Figure 12).

The second suite, displaying a sharp to transitional contact with the coarse-grained suite, is medium- to fine-grained and is characterized by the relative abundance of biotite and the presence of rare amphibole, sometimes in coarse crystals. Biotite is generally present in small “flakes”, although some



Figure 14 - Mingling (lower part of the picture) and layering (upper left) between tonalite and granodiorite from the second suite (Western Gelta, area N of Rauchkofel, 2500m asl).



Figure 15 - Interlayering of medium- to finegrained granodiorite and tonalite.

“book” crystals can be observed in the contact zones. Rocks of this suite range in composition from tonalite to granite and do not any contain garnet. The contact between tonalitic and granodioritic rocks is mainly transitional, with evidence of mingling (Figs. 13, 14) and interlayering (Figs. 14, 15).



Figure 16 - Sharp contacts between granodiorite and tonalite from the second suite. Dikes of evolved granodiorite magma cut and disrupt the (partially) crystallized tonalite (South of Riesernock, along the Hartdegenweg, 2320m asl).

Sharp contacts and dikes of granodiorite intruding and dismembering the tonalite are also observed (Figure 16).

The third suite, located in the central-eastern part of the pluton and mostly surrounded by rocks of the second suite, is medium- to fine-grained and displays a rather homogeneous leuco-granodioritic composition. Biotite, in accessory quantities, is the only mafic mineral, and K-feldspar appears in centimetric individuals. Contacts with rocks of the previous suite are sharp (Steenken et al., 2000).

Chemical characters of the Vedrette di Ries rocks and genetic hypothesis

The intrusive rocks of Vedrette di Ries show a calcalkaline character. They have invariably low TiO_2 content (<0.8 wt%), high Al_2O_3 and low FeO/MgO ratio.

From the geochemical point of view the three suites (Figure 17) can be distinguished based on their Ca, Sr, Rb (Figure 18) contents and trends (Bellieni et al., 1978).

Further investigations pointed out that, based on their REE contents, rocks of Vedrette di Ries can be subdivided into two main groups characterized by low (<1.1) Tb_N/Yb_N and high Tb_N/Yb_N values (Figure 19).

According to Bellieni et al. (1981) the rock series represents the product of a two-stage crystal/liquid fractionation starting from one and the same parent magma. During a first stage, at high pressure, separation of hornblende + garnet lead to magmas with high Tb_N/Yb_N , representing the ancestor of each suite. These magmas, during their rise at lower pressure, underwent a second stage of fractional crystallization with separation of hornblende + plagioclase, and then evolved towards Sr-poor compositions. Processes of contamination with crustal material and separation of accessory phases had an important role in determining the high $^{87}Sr/^{86}Sr$ values and the uneven distribution of some trace elements (Bellieni et al., 1981).

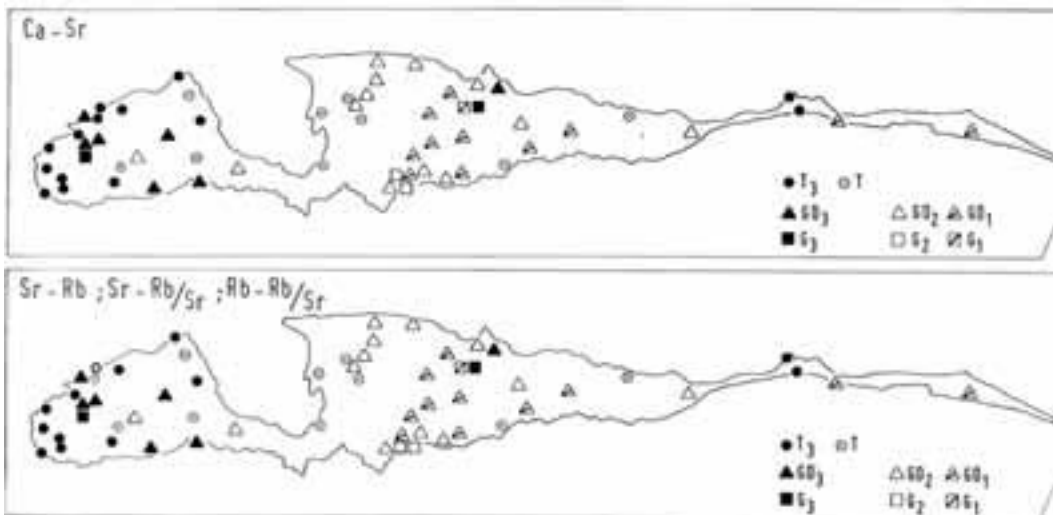


Figure 17 - Areal distribution of the three different suites of rocks in Vedrette di Ries as identified by the Ca-Sr and Rb-Sr variation diagrams (taken from Bellieni, 1978).

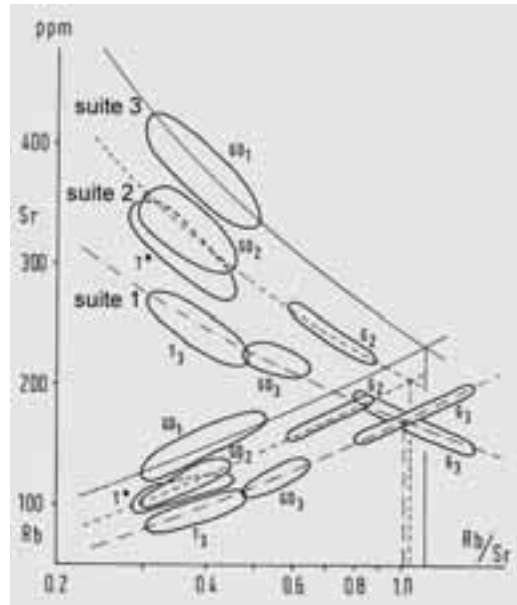


Figure 18 - Cumulative diagram of Rb and Sr vs Rb/Sr taken as a differentiation index. The three suites of rocks define different trends. The intersection of Rb and Sr curves for each suite takes place at different Rb/Sr values. Suite T3-GD3-G3 corresponds to the first, coarse-grained, garnet bearing suite. Suite T²-GD2-G2 corresponds to the second, fine-to medium-grained suite. GD1 represents the third, central, homogeneous leuco-granodiorite. (Taken from Bellieni, 1978).

Mafic microgranular enclaves (MME) are common. They are abundant in the first, coarse-grained suite and occasional in the third granodioritic suite. Their abundance decreases with the increasing SiO₂ of the host and their composition reflects that of the host, the most mafic enclaves being observed in most mafic hosts. Garnet is restricted to MME sampled within the garnet-bearing suite. Based on their petrographic, geochemical and isotopic characters, Bellieni et al. (1989) argued that MME represent blobs of mafic magma whose original composition was modified by interaction with the host magma (Figure 20). MME are therefore good strain markers (Figure 21).

Metamorphic xenoliths are locally abundant not only close to the country rocks, but also in some central areas of the magmatic body. Small metamorphic "surmicaceous" xenoliths are particularly abundant in rocks from the second suite. Assimilation of country rocks actually played an important role in the evolution of these magmas, as indicated by their high initial ⁸⁷Sr/⁸⁶Sr isotopic composition and by its wide

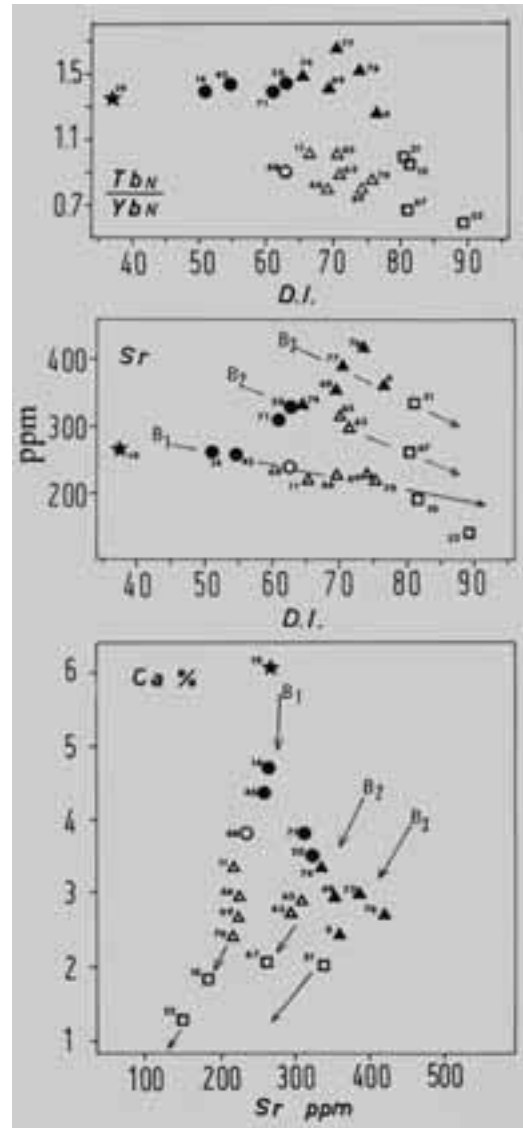


Figure 19 - Two main groups of rocks can be identified in Vedrette di Ries based on their Tb_N/Yb_N: rocks with low (<1.1) Tb_N/Yb_N values (empty symbols), and rocks with high Tb_N/Yb_N (filled symbols). In the Sr versus D.I. (Differentiation Index) and Ca vs Sr diagrams, rocks with high Tb_N/Yb_N plot at the origin of each of the three distinct geochemical trends of Vedrette di Ries (reported as B1, B2, B3). Stars: diorite; circles: tonalite; triangles: granodiorites; squares: granite.

variational range (Borsi et al., 1979).

All suites are cut by late acidic and mafic dikes and veins (Figure 22). Acidic dikes range from centimetric to metric, have an overall E-W orientation, and often



Figure 20 - Mafic microgranular enclave surrounded by a centimetric reaction halo.



Figure 21 - Example of late flattening on a mafic microgranular enclave and an aplitic dike.

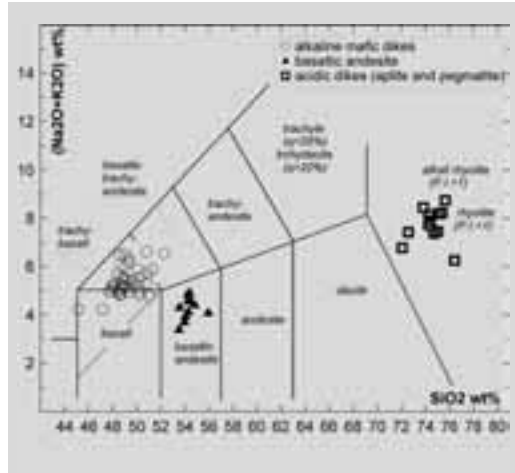


Figure 22 - TAS classification diagram for acidic and mafic dikes within Vedrette di Ries Pluton (Fioretti et al., unpublished).

constitute swarms of subparallel individuals that only seldom intrude the metamorphic country rock. Aplitic dikes are more common than pegmatitic ones and may contain spessartine garnet. They represent the latest magmatic activity linked to the emplacement and evolution of Vedrette di Ries.

Lamprophyric dikes with a dominant N-S orientation, show sharp contacts with the intruded host (Figure 23).

Mafic dikes are not part of the Vedrette di Ries magmatic cycle. They cut both the plutonic rocks, including aplite and pegmatite dikes, and the metamorphic country rocks. They are centimetric to decametric and range in composition from trachy-basalt to basaltic andesite (Figure 21). Both calcalkaline and shoshonitic products are present, sometimes even within the same dike (Schiavon, unpublished degree thesis), where pristine shoshonitic magma is intruded and disrupted by younger calcalkaline magma (Figs. 24 and 25)

Mafic dikes are commonly found also in the surrounding basement. They belong to a widespread "andesitic" l.s. dike activity that interested not only the Austroalpine, but also the Southern Alpine and Penninic units (Gatto et al., 1976). K-Ar age determinations on a lamprophyric dike within Vedrette di Ries yields an age of 26.3 ± 3 Ma (Steenken et al., 2000).



Figure 23 - Mafic dike with magmatic lineation along the wall (S-SE of Rifugio Roma).

Geochronology

Borsi et al., (1979) reported a whole rock Rb/Sr age for Vedrette di Ries of 30 ± 3 Ma and $^{87}\text{Sr}/^{86}\text{Sr}$ with an initial ratio of 0.709. Higher values of the initial $^{87}\text{Sr}/^{86}\text{Sr}$ (up to ca. 0.720) were obtained from other batches of magmas and from some granite (Borsi et al., 1979, Cavazzini et al., unpublished data). Field evidence indicates that Vedrette di Ries is younger



Figure 24 - Veining of a mafic dike by more evolved magma. The horizontal lines are glacial stripes.



Figure 25 - Pristine magma disrupted by younger calcalkaline magma within the same dike.

than the acidic porphyritic dikes outcropping in the surrounding basement (Cescutti et al., 2003). These dikes have been correlated (Cescutti et al., 2003) with those outcropping at the Austroalpine-Penninic limit north of Rensen (Figure 3), dated at 30.9 ± 0.2 Ma by Müller et al. (2000). The late lamprophyric dikes cross-cutting Vedrette di Ries are 26.3 ± 3 Ma (Steenken et al., 2000).

Metamorphism

In the region between the Tauern Window and the Periadriatic Lineament, the Austroalpine basement of the Eastern Alps forms an E-W trending belt, divided into three blocks by two major tectonic lines: the Deferegggen-Anterselva-Valles (DAV) line and the Kalkstein-Vallarga (KV) line (Borsi et al. 1978).

Unlike the other two blocks, which display an essentially pre-Alpine tectono-metamorphic history, the block north of the DAV line was involved in the Alpine metamorphic cycle (Borsi et al., 1978): its polymetamorphic history can be summarized as follows:

- 1 - "Caledonian" metamorphism of undetermined P-T conditions (Borsi et al., 1973; Hammerschmidt, 1981)
- 2 - Variscan high grade metamorphism and anatexis at $P = 6 \pm 1$ kbar and $T = 650$ °C (Stöckhert, 1985, 1987;

Schulz, 1997);

- 3 - Eo-Alpine metamorphism under relatively high-P/low-T conditions (7.5 ± 1.5 kbar and 450 ± 50 °C, Stöckhert, 1984, 1987; Prochaska, 1981);

- 4 - "Main-Alpine" ("Tauern") metamorphism under lower greenschist facies conditions (Sassi et al., 1980);

- 5 - Oligocene contact metamorphism in the aureole of the Vedrette di Ries pluton (Bianchi, 1934; Prochaska, 1981; Schulz, 1989; Cesare, 1994a, 1999a): the last metamorphic event recorded in the area.

Metamorphism was accompanied by intense deformation during both the eo-Alpine (Stöckhert, 1987) and the late-Alpine events (Kleinschrodt, 1987). Oligo-Miocene dextral and sinistral mylonites are widespread throughout the area, pointing to an intense coaxial component of deformation in front of the Dolomite indenter (e.g. Müller et al., 2001). Discrete mylonite zones of considerable thickness and lateral continuity occur far from (and north of) the DAV line, in addition to numerous smaller and discontinuous ones (Mancktelow et al., 2001).

However, parts of the block escaped the Alpine structural reworking (not the metamorphic overprint) preserving pre-Alpine structures and metamorphic relict assemblages (Borsi et al., 1978). One of these areas is located south of the Vedrette di Ries tonalitic

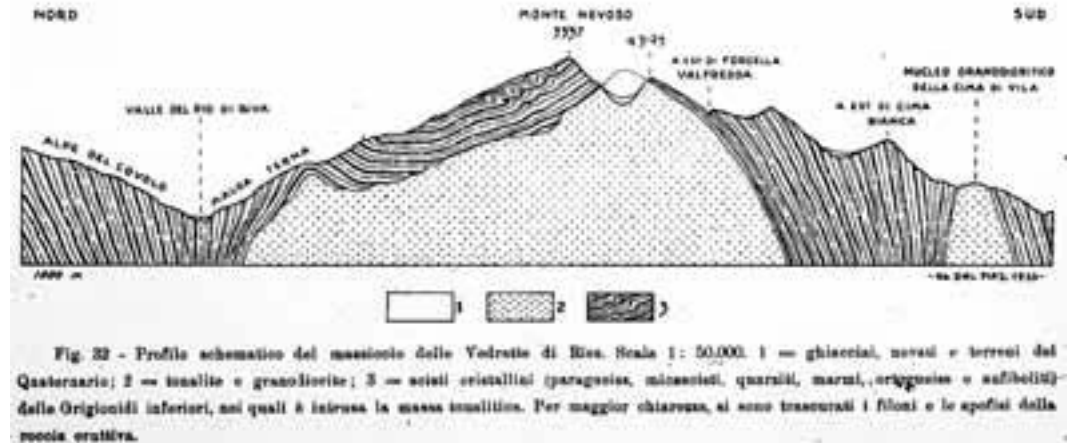


Figure 26 - North-south cross-section across the Vedrette di Ries pluton (from Dal Piaz, 1934) showing the antiformal structure in the country rocks.

pluton; here metapelitic schists and migmatitic paragneisses are dominant, with minor interbedded layers of pegmatite gneiss, marble, quartzite and amphibolite. The well-developed Variscan metamorphic layering, isoclinally folded, strikes E-W and dips south 30° to 60°; the overall structure represents the southern flank of a kilometer-sized antiform quasi-concordant with the pluton margin (Figure 26).

The contact aureole of the Vedrette di Ries tonalite is approximately 1.5 kilometres wide and has been divided by Cesare (1992) into five mineralogic zones, which correspond to type 2bii of Pattison & Tracy's (1991) facies series scheme. The pressure of contact metamorphism is estimated at 2.5-3.75 kbar (Cesare, 1994a, using the Holdaway's (1971) Al_2SiO_5 triple point of, with maximum temperatures of 600-620°C. A weak deformation, occurring as a reactivation of the earlier main foliation, accompanied the contact metamorphism and is localized in the zones of highest metamorphic grade, close to the pluton contact.

Field trip itinerary

The area we are going to visit is completely enclosed in the "Naturpark Rieserferner-Ahrn".

The Park is the largest one in Southern Tyrol and was founded 13 years ago. It constitutes a successful example of protecting a wide area not by imposing restrictions that eventually prevent the native population from using it, but by pursuing a considerate policy of integration and sustainable development. The Park is not only accepted by the population but also protected and actively maintained.



Figure 27 - "May the Lord be praised": carved block of tonalite, Franziskusweg, Naturpark Rieserferner-Ahrn.

The mountains, woods, water, and grazing areas are home for the people living here. Cultural traditions are proudly cultivated and transmitted. The beauty of these places testifies to the care and love of the local population for their homeland, and for which God is also gratefully acknowledged (Figure 27). Please, be considerate. Whereas you are certainly allowed to take some samples with you, we kindly request you not to leave any major trace of your passage.

DAY 1

Brunico (Bruneck) - Campo Tures (Sand in Taufers) - Riva di Tures (Rein in Taufers) - Sorgiva (Ursprung) valley - Rifugio Roma (Kasseler Hütte).

a) Riva di Tures valley (Reintal): a visit to the tonalite quarries and introduction to the petrology and

geochemistry of the composite pluton of Vedrette di Ries. b) Sorgiva-Ursprung valley: walk to the northern contact of the pluton. Outcrops of mylonites at the contact and intensely deformed tonalite. Discussion of the structural and chronological relationships between emplacement and ductile deformation, and of the role of the northern mylonite zone. c) A walk along the Hartdegenweg to the Rifugio Roma (2275 m a.s.l.): outcrops of various facies of the tonalite. Strain gradient in the tonalite, mingling and injection relationships between fine-grained and coarse-grained facies, aplitic, granitic and lamprophyric dikes cutting the main body.

Stop 1:

Road between Campo Tures - Riva di Tures (c. 1150m a.s.l.). Quarries of tonalite along the Rio di Riva Valley. Coarse-grained, Grt-bearing tonalite and granodiorite. Contact with the medium- to fine-grained granodiorite without garnet. Granite and aplitic dikes. Petrogenetic implications of the presence of garnet will be discussed.

Garnet is one of the main features of the coarse-grained suite (Figure 10). In calc-alkaline magmas garnet is rare, but not unusual; experimental work by Green (1972) and Green & Ringwood (1972) have demonstrated that it forms at pressure conditions > 10 Kbar. However, the observations that magmatic garnet-bearing rocks in Vedrette di Ries represent a sort of belt around the pluton close to the contact with the metamorphic country rocks, and that all along the contacts magmatic rocks contain metamorphic xenoliths with abundant garnet, suggested that garnet in the Vedrette di Ries plutonic rocks might exclusively be linked to the assimilation of country rocks. This problem was addressed by Bellieni et al. (1979) and recently reconsidered by Bassani (unpublished degree thesis, 1996).

Garnet in Vedrette di Ries tonalite and granodiorite is up to 2 cm wide and is generally idiomorphic. It is typically surrounded, and sometimes totally replaced, by a reaction rim made up of fine-grained plagioclase \pm biotite \pm quartz (\pm amphibole) (Figure 28). Preserved individuals show concentric shells of Pl \pm Qtz \pm Bt \pm Hbl inclusions, likely representing samples of the coexistent crystallizing magma. Garnet is zoned with a wide, rather homogeneous, nucleus of almandine composition (Alm 50-70%, Sps 2-10%) and a narrow more spessartine-rich rim (Alm 35-40%, Sps 12-15%). The core composition of garnet is independent from the rock, i.e. core composition of garnet in diorite, tonalite and granodiorite is the same



Figure 28 - Subhedral garnet with atoll inclusions (amphibole \pm plagioclase \pm biotite \pm opaque minerals), surrounded by a thin reaction rim.

(Fig 29).

The compositional range of rims is more scattered, possibly due to different degrees of interaction with distinct magmas.

The composition of included minerals shows some systematic differences compared to that of the same phases occurring in the rock. While plagioclase in the rock shows a marked zoning with bytownite core and up to oligoclase rim, plagioclase within garnet lacks the An-poor external rim, and its intermediate zones are very thin. Amphibole in garnet is Fe-hornblende and is Al-richer than the Mg-hornblende of the rock. On the other hand, the composition of biotite inside garnet and within the rock is almost the same. Petrographic and mineral-chemical characters fit the hypothesis that minerals in inclusions formed by crystallization of portions of the magmatic liquid trapped in garnet during its crystallization (Figure 30). The composition of minerals in the reaction rim is rather homogeneous. Plagioclase is oligoclase, and amphibole composition straddles the

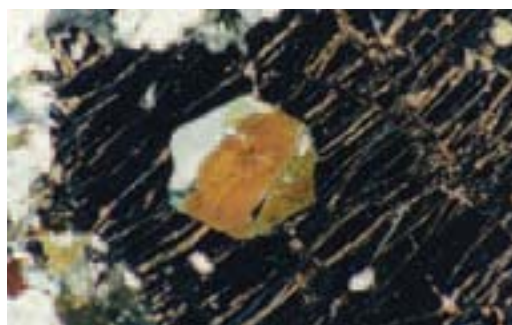


Figure 30 - Inclusion in garnet. The shape of the inclusion, a negative garnet crystal, and the composition of the mineral phases suggest that included minerals crystallized from a portion of trapped magmatic liquid.

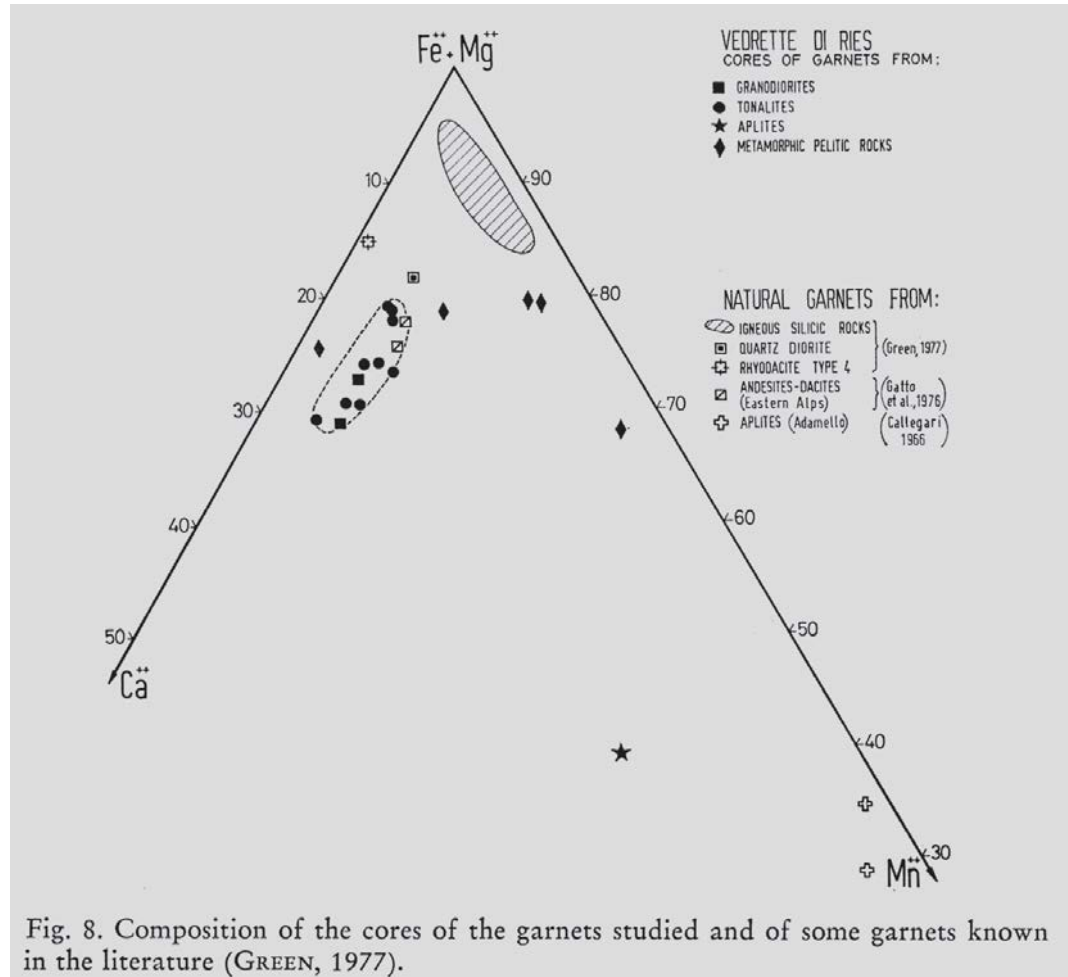


Figure 29 - Composition of garnet core from tonalite and granodiorite (full squares and circles), from the country metamorphic rock (diamonds) and from aplitite (star). Magmatic cores define an elliptical coherent field with rather constant spessartine contents.

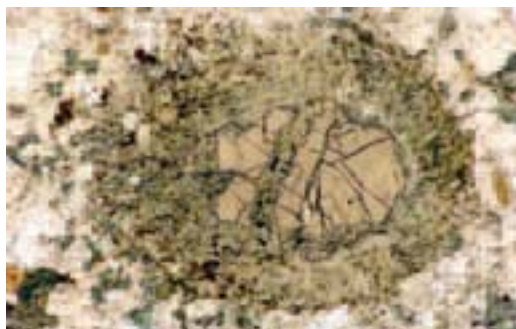


Figure 31 - Reaction border around garnet. The width of the reaction border ranges from a thin rim to the complete substitution of the original garnet.

fields of Fe-hornblende and Mg-Hornblende.

Taking into consideration the garnet cores, Bellieni et al. (1979) estimated that garnet was in equilibrium with liquidus at $P > 10 \text{ Kb}$, $T < 950^\circ\text{C}$ and water content of approximately 5%. Garnet either formed or grew on relics during magmatic crystallization, and reached instability conditions only during a later stage, as suggested by the presence of a reaction border (Figure 31).

The instability of the garnet, accompanied by a marked plagioclase zoning (Bellieni et al., 1976), is presumably linked to a relatively rapid uprising of the magma towards shallower crustal levels (ca.

2 Kb), where the magma eventually emplaced. An identical conclusion was independently reached by studying the crystallization of the cotectic minimum of the granitic rocks (Bellieni, 1977). Contact mineral assemblage of the country rocks (Bellieni, 1977; Cesare, 1992) further confirms the final emplacement level of the Vedrette di Ries magma.

Stop 2:

Path 8c, 1735m a.s.l. Foliated, coarse-grained tonalite just before the bridge over Rio di Riva. Foliations dip to the N-NW of 50-60°.

Stop 3:

Path 8c from Riva di Tures (Loc. Säge) to Ursprungalm, along the river, 1850m a.s.l. Strongly foliated country rocks at the northern intrusive contact.

The mylonitic paragneisses contain both layer-parallel and discordant dikes and apophyses of coarse-grained tonalite. These relationships suggest that mylonitic deformation was active in this area during the initial stages of pluton emplacement, and that it stopped before the final stages of emplacement.

Along path 8c to Ursprungalm several aspects and phenomena deserve consideration:

- 4) at 1900m a.s.l: paragneisses with transposed tonalite injections along mylonitic foliation;
- 5) from 1900m to 2100m a.s.l: the path climbs up to the north of a hill mostly made of amphibolites;
- 6) at 2290m a.s.l: the amphibolites and paragneisses are crosscut by a porphyritic dike (Cescutti et al., 2003). The dike is c. 3 m thick, and is strongly sheared within the dominant mylonitic foliation. This kind of dikes, of granitic composition, never crosscuts the Vedrette di Ries plutonic rocks, and is therefore older. Similar rocks, named "porphyritic tonalites" have been dated at 30.9 ± 0.2 Ma by Müller et al. (2000).

The mineral assemblage of this kind of dikes is plagioclase, quartz, K-feldspar, muscovite, and biotite. Garnet, allanite, apatite, opaque minerals and zircon are present in accessory quantities. Based on petrographic evidence (garnet composition and zoning, its presence inside the core of zoned plagioclase, overgrowth of new garnet around individuals not included in plagioclase, partial resorption and subsequent crystallization of new plagioclase), and their chemical signature, a genesis by partial melting of deep crustal material and an emplacement at shallow levels following a polybaric

crystallization was proposed for these dikes (Cescutti et al., 2003).

Stop 4:

Path 8a to Rifugio Roma, 2320m a.s.l. The well-exposed northern contact of the pluton.

Mylonitic paragneisses with transposed tonalitic dikes. The country rocks in this area are largely made of mylonitic paragneisses, containing numerous veins and apophyses of coarse-grained tonalite, transposed and boudinaged within the foliation (Figure 32, see also Steenken, 2002). In the paragneisses, biotite and fibrolitic sillimanite occur in the synkinematic assemblage. As sillimanite occurs in this area only as a product of contact metamorphism, we can conclude



Figure 32 - Small tonalitic dike transposed in the foliation of country rock paragneisses. In the paragneiss, the foliation is outlined by synkinematic sillimanite (fibrolite).



Figure 33 - Boudinage of a dm-thick amphibolite layer at the northern intrusive contact of the Vedrette di Ries tonalite, in the upper Val Sorgiva.

that the mylonitic foliation developed during contact metamorphism, i.e., that it was synchronous with pluton emplacement.

Amphibolites, metacarbonates and calc-silicate rocks at the immediate contact. As also observed in the



Figure 34 - Remnants of the pluton's roof (darker colour) on top of the Sprone delle Vedrette Giganti.

lower Val Sorgiva, country rocks at the immediate contact of the tonalite are often composed of fine-grained, biotite-bearing amphibolites, marbles and calc-silicate rocks. The latter contain garnet, epidote and clinopyroxene, and may develop a very coarse grain-size. As in the metapelitic mylonites, a strong deformation can be observed also in these rocks, with beautiful examples of boudinage in the amphibolite layers (Figure 33).

Boudinage of tonalite within the enclosing paragneisses points to a more competent behaviour of the tonalite, and hence to deformation in the solid state. This area records the largest strain of the entire pluton and it is characterised by sinistral shearing along a steep, E-W striking zone, displaying subhorizontal stretching lineations. Magmatic fabrics are entirely overprinted by greenschist facies deformation. However, melt-bearing shear bands are found locally, suggesting a continuous deformation from the magmatic to the solid state. Aspect ratios of enclaves of ~ 10:1 rapidly decrease to ~ 3:1 towards the pluton's interior (Wagner et al., in review).

Stop 5:

Path 8 to Rifugio Roma, c. 2400m a.s.l. A ten-metre-sized zone of mingling of coarse- and fine-grained tonalite at the northern contact.

Again, the country rocks at the contact are characterized by the presence of marbles and calc-

silicate rocks. The coarse-grained tonalite contains some garnet here.

Stop 6:

Path 8 to Rifugio Roma, c. 2320 m asl. Sharp contacts between medium- to fine-grained tonalite and granodiorite.

Dikes of evolved granodiorite magma cut and disrupt the already crystallized tonalite (see Figure 16). The foliation is discordant to the wall of the dikes.

From the Rifugio, a panoramic view towards the eastern sector of the massif, with large remnants of the pluton's roof (Figure 34) on top of Sprone delle Vedrette Giganti (Riesernock). That is the only location where the divariant KNASH contact metamorphic assemblage Ms-Kfs-Qtz-Sil (or "second sillimanite" zone) has been observed in paragneisses, helping constrain the P-T conditions of contact metamorphism (Cesare, 1992, 1994a).

DAY 2

Rifugio Roma and surroundings.

Aplitic and lamprophyric dikes post-dating the main intrusion of Vedrette di Ries. Ice-polished outcrops at the front of the Monte Nevoso Glacier: intrusive contact between the tonalite and the metapelites of the Austroalpine basement; synintrusive deformation

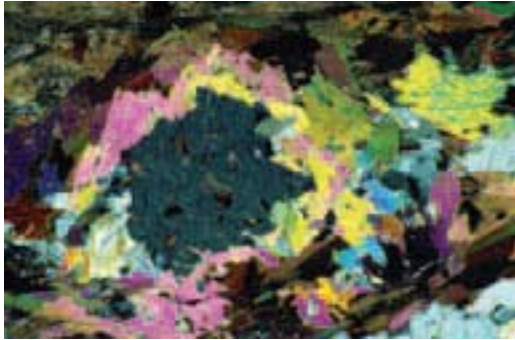


Figure 35 - Replacement of andalusite by coarse-grained, prograde muscovite. Sillimanite (fibrolite) is the stable Al_2SiO_5 polymorph, and occurs in the matrix around the nodular pseudomorph.



Figure 36 - The reaction of staurolite to hercynite accompanies the topotactic replacement of andalusite by sillimanite in the metapelites at Stop 2. Taken from Cesare (1994a).

and contact metamorphism of the country rocks; oligocene Grt-Ms-Tur-Ber-bearing pegmatites.

Stop 1:

Swarm of mafic, lamprophyric dikes with a general N-S direction. Sharp, brittle contacts, intrusion of thin lamprophyre apophyses along fracture zones, and presence of angular granodioritic xenoliths within the dikes testify for their late emplacement. Chilled margin and magmatic foliation are well developed in wider dikes (Figure 23). Subsequent intrusions along the same feeder are testified by network of less mafic veins (Figure 24) that eventually lead to the disruption of the already solidified mafic magma (Figure 25). Spherical to ameboid geodes of acicular amphibole in a medium grained matrix within the mafic dikes suggest a crystallization at high P_{H_2O} .

Stop 2:

Ice-polished rocks at the base of the Tristenferner glacier, c. 1800 m south of Rifugio Roma, 2550 m a.s.l.. Here is one of the best exposures of the intrusive contact between underlying fine-grained tonalite and overlying metapelitic country rocks, thoroughly affected by contact metamorphism and synintrusive deformation. Rather than a sharp surface, the contact is an intrusion/interaction zone of some tens of metres in thickness, where several layer-parallel tonalite injections are observed. Overall, the contact is generally concordant with the country rocks' foliation, and dips c. 30° to the north. This area can be considered a part of the pluton's roof.

The country rocks are mostly migmatitic paragneisses (Hofmann et al., 1983) characterized by a Qtz-Pl-Ms-Bt-And-Sil-St-Spl-graphite assemblage. Although easily recognized in the hand specimen, staurolite and andalusite are metastable relicts of lower-grade contact metamorphism, and are transformed into

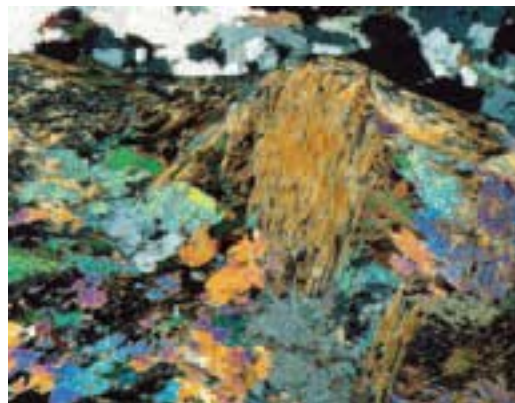


Figure 37 - Contact metamorphic prismatic sillimanite bent and wrapped by fibrolite-bearing foliation.



Figure 38 - Tourmaline and garnet in the pegmatites of likely Oligocene age.

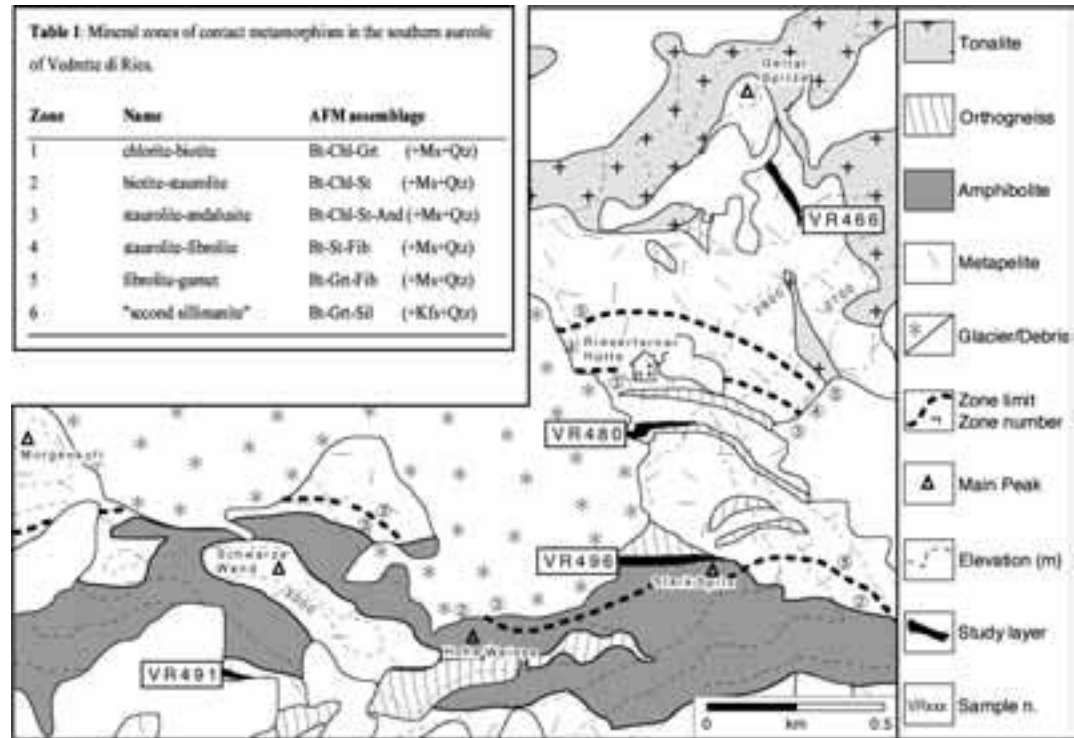
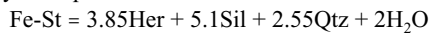


Figure 39 - Simplified geological map (after Mager, 1985) of the southern aureole of Vedrette di Ries, with location of the rock layers studied and respective sample numbers. Mineral zones as in Table 1 (inset).

nodular pseudomorphs consisting of coarse-grained muscovite (Figure 35), topotactic prismatic sillimanite and hercynite (Figure 36).

In the above microstructures, Cesare (1994a) has formulated the decomposition of staurolite to hercynitic spinel as:



and has constrained the P-T conditions of contact metamorphism at 2.5-3.75 kbar and 585-655 °C.

Like in the upper Val Sorgiva, the well-developed foliation of the paragneisses is outlined by fibrolitic sillimanite. In addition, prismatic sillimanite appears to have been bent and wrapped by the foliation (Figure 37). Therefore, the foliation of the country rocks developed, or was reactivated, during the contact metamorphism.

The Vedrette di Ries pluton is typically poor in pegmatitic rocks. Among the few pegmatites which are likely to be related to the Vedrette di Ries intrusion are some meter-thick discordant dikes which occur in this outcrop. Although in this location one cannot observe the pegmatites which intrude the tonalites, the structural features suggest that these rocks post-date

contact metamorphism. In fact, the pegmatites form a set of parallel injections at a high angle compared to the foliation of the host paragneisses. Along with quartz and feldspars, these pegmatites contain biotite, muscovite, garnet and tourmaline (Figure 38). Light green beryl has also been discovered here.

The fine-grained underlying tonalite is strongly oriented, with elongated microgranular enclaves. It also shows widespread cataclastic deformation and low-temperature alteration, with development of abundant chlorite and epidote.

This area is also particularly interesting for the observation of the geomorphological effects of the little ice age (1450-1850), such as huge lateral and terminal morains, ice-polished rocks and small glacial lakes. The glaciers of the Vedrette di Ries massif are undergoing a dramatic retreat (Santilli et al., 2002).

Afternoon: descent to Riva di Tures and trip to Anterselva.

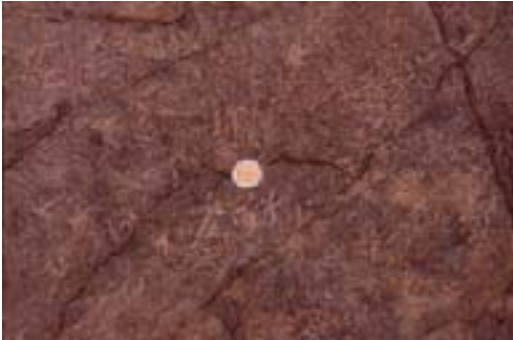


Figure 40 - Hand specimen of a graphitic schist from lower Zone 3, with abundant coarse-grained andalusite porphyroblasts.



Figure 41 - Metapelitic schist from upper Zone 3. The light brown to orange nodules are polycrystalline aggregates of staurolite. See Figure 42 for a microscopic view of an aggregate from this rock.

DAY 3

Rifugio Forcella Valfredda (Rieserfernerhütte) and surroundings.

Contact metamorphism and related phenomena in the southern aureole of Vedrette di Ries. Profile of the outer, regionally metamorphosed (Variscan and Alpine) metapelites up to the intrusive contact; observation of the well-developed St-And-Sil zoneography; discussion of thermobarometric constraints to depth of emplacement. The Andalusite-bearing veins and their fluid inclusions: a marker of fluid-rock interactions during contact metamorphism.

Participants will walk along a S-N oriented profile covering the whole contact aureole up to the intrusive contact with the fine-grained tonalite. We are not dividing the day into stops, as there would be too many. However, we will refer to the maps provided herewith. Here follow the detailed descriptions of the two main objects of this part of the field trip: the contact metamorphism and its zoneography and the andalusite-bearing veins.

Contact Metamorphism at Vedrette di Ries

The area of Rifugio Forcella Valfredda is the ideal place to observe the effects of contact metamorphism induced by the tonalite of Vedrette di Ries. The southern aureole is mainly composed of metapelites, but orthogneisses, quartzites, amphibolites and marbles also occur. As previously stated, these rocks belong to the Austroalpine basement to the north of the DAV line, and have undergone a complex and polyphase metamorphic evolution before being

affected by the Oligocene contact metamorphism. We will focus our attention on the effects of contact metamorphism on metapelitic lithologies.

The southern contact aureole of Vedrette di Ries has been divided into five mineralogical zones (Table 1, Figure 39, Cesare 1992) which developed at c. 3 kbar. In the metapelites, the most evident minerals of contact metamorphic origin are the abundant and very coarse andalusite (up to 10 cm in length, Figure 40), and the unusually fine-grained staurolite, which often occurs in polycrystalline nodules (Figure 41).

Another peculiarity of this area is that layers of a distinctive rock type crop out in at least four localities, at variable distance from the intrusive contact (Figure 39). These rocks allow for reconstruction of the multi-stage pseudomorphic replacement of a primary garnet: here follows a summary of the microstructural study and of the main conclusions outlined by Cesare (1999a, b), where further details and an updated reference list can be found. The layers have a thickness of < 20 m, and consist of fine-grained mica-schists with a marked millimetric compositional layering, with abundant quartz-rich ribbons, probably the result of mylonitic deformation. The foliation wraps around lensoid domains in which garnet, kyanite, staurolite, andalusite and muscovite are dominant in turns. The systematic distribution of Al_2SiO_5 polymorphs in the aureole, and the resulting isograd pattern (Figure 39), indicate that during the contact metamorphic event only the layer closest to the contact (i.e. sample VR466) reached temperatures sufficient for the crystallization of sillimanite. It follows that in all the other layers any occurrence of sillimanite is attributed

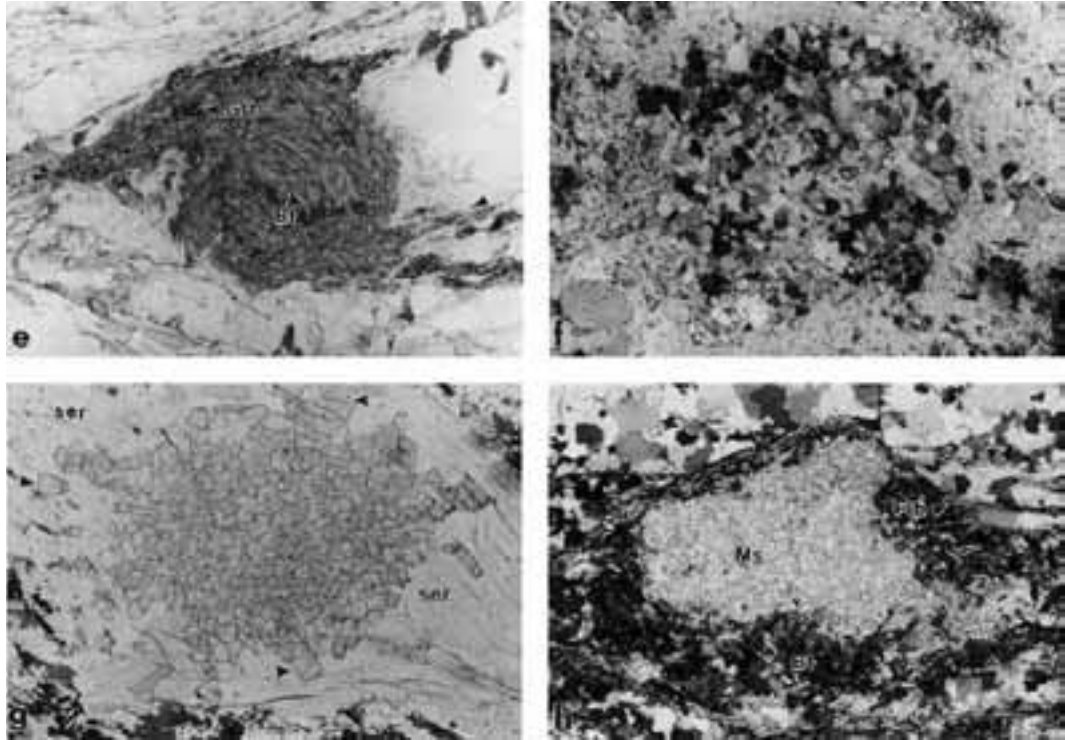


Figure 42 - Close-up views of nodules from each sample. e: VR491. Round aggregate of microgranular kyanite with minor biotite, ilmenite and garnet. Two kyanite-rich asymmetric tails (arrows) extend in the subhorizontal main foliation. Plane-polarized light (PL), width of view (wv)= 6.5 mm. f: VR496. Nodule of kyanite and staurolite. Kyanite occurs at the core of most staurolite crystals (stars). Crossed polars (CP), wv = 6.5 mm. g: VR480. Monomineralic nodule of staurolite in a sericite aggregate (ser). Note (arrows) the coarser grain-size of staurolite on the periphery of the aggregate, or isolated in the sericite matrix. Sericite around nodule (lower right) shows preferred orientation with incipient shear band cleavage. This suggests reactivation of the main foliation during contact metamorphism. PL, wv = 6.5 mm. h: VR466. Decussate monomineralic aggregate of muscovite wrapped by folia of biotite and fibrolite. PL, wv = 6.5 mm.

to earlier metamorphism. Both field appearance and microstructural characteristics suggest that these rocks, although showing different mineralogical composition at each locality, may represent the same primary rock type (the same folded layer?), variably transformed during the complex metamorphic evolution of this area.

Sample description

Four samples have been chosen as representative of the rock type at each location, and used for microstructural, bulk chemical, and mineral chemical analysis. See Figure 39 for their locations.

VR491: from Zone 1 (chlorite-biotite) of contact metamorphism. The sample furthest from the intrusive contact. It is a silvery, muscovite-rich schist, with abundant nodular aggregates of kyanite, typically <5mm in diameter. Garnet is present, either as isolated porphyroblasts, or associated with kyanite

in the aggregates.

VR496: from the outer Zone 2 (andalusite-staurolite). Light gray, strongly layered but massive schist, rich in garnet porphyroblasts and nodules of fine-grained, brown staurolite. Staurolite often forms coronas around garnet. Andalusite crystals, up to 3 cm in length, occur in the muscovite-rich layers of the matrix.

VR480: from the inner Zone 2. A dark-brown rock, with orange-brown nodules composed of microgranular staurolite up to 1 cm in diameter. Coarse porphyroblasts of andalusite occur in the mica-rich layers that contain biotite, muscovite and staurolite. Quartz ribbons and rods may reach one cm in thickness.

VR466: from Zone 4 (sillimanite-garnet). The sample location is very close (approx 50 m) to the pluton. This massive rock is almost black, owing to the biotite-rich matrix that forms layers alternating with

quartz ribbons and fibrolite-rich folia. Pink andalusite porphyroblasts are abundant, whereas the scarce muscovite is mainly concentrated within mm-sized nodules.

Figure 42 compares the general textural appearance of the four samples at the thin section scale. The most striking similarities are the presence of nodular aggregates of comparable size, wrapped around by the matrix, and the occurrence of quartz-rich ribbons. In addition, all rock samples are graphitic, and contain tourmaline crystals with similar, complex zoning. A progressive grain-size coarsening of matrix phases (e.g. biotite and muscovite), aggregate phases (e.g. staurolite), as well as nodular aggregates themselves, can be observed, even in hand specimens, in the transition from sample VR491 to sample VR 466. This is consistent with the higher temperatures and the longer duration of contact metamorphism in the samples closer to the pluton.

A model for the evolution of a primary garnet site

The above microstructural information allow for reconstruction of the complex textural evolution of a primary garnet site, now represented by the nodules. Preservation of the subspherical shape of garnet was favoured by the very low strain experienced by these rocks after garnet crystallization, which resulted in the static growth of minerals in all the subsequent metamorphic events. The textural sequence can be divided into five (or six) stages:

The Garnet Stage (VR491, VR496) - This is the earliest microstructural stage, with garnet porphyroblasts of < 1 cm diameter wrapped by the micaceous layers. Inclusions in garnet consist of quartz, biotite, ilmenite and muscovite, and provide no information regarding the metamorphic history of the metapelite prior its crystallization.

The Fibrolite Stage (VR491, VR496) - Although there is no direct evidence for a stage where nodules were composed of fibrolite, several indications point to this occurrence. They include: i) the presence of fibrolite in close association with the nodules, formerly occupied by garnet; ii) the radiating arrangement of needles, diverging from the nodule; iii) the presence of biotite with exsolution of ilmenite and iv) the proposed crystallization sequence, in which fibrolite predates kyanite. These data are suggestive of the high-T reaction of garnet to fibrolite + Ti-rich biotite. Thermodynamic modelling of this reaction predicts a complex behaviour for garnet, which then may dissolve, grow or not react at all depending on the local configuration of the matrix. This is in

agreement with the presence, in sample VR491, of untransformed garnet crystals adjacent to partially or completely pseudomorphed ones.

The Kyanite Stage (VR491, VR496) - This is represented by the nodules of microgranular kyanite which maintain their primary shape of garnet, but are not thought to have replaced it directly. The very fine grain-size of kyanite in the nodules is an anomalous feature for metapelites; this peculiarity, and its possible cause, is discussed below.

As it is not clear whether sericite pre-dates kyanite or is coeval with it, the possibility of a further stage pre-dating the Kyanite stage, and represented by sericite crystallization (the Sericite stage), has to be considered. Sericite would form “shimmer aggregates” upon replacing fibrolite, and leave relict needles within quartz and muscovite adjacent to nodules.

The Staurolite Stage (VR491, VR496, VR480) - This stage, initiated in sample VR491 and completed in sample VR480, produces the nodules of microgranular staurolite. Microstructures indicate that staurolite crystallization is coeval with that of andalusite, or that it commenced slightly before, and continued during, andalusite growth. As a consequence, the staurolite stage is related to the contact metamorphism.

The Muscovite Stage (VR466) - This is the final stage, in which decussate aggregates of muscovite replace staurolite. Although this kind of pseudomorph is common during retrograde metamorphism, even in this area, in this sample it has been shown to represent a prograde feature. Similar prograde pseudomorphs of muscovite after staurolite were first described by Guidotti (1968) in a regional metamorphic context. The inferred age of the stages can be summarized as follows:

Stage	Age	Setting
Grt	Variscan	Regional
Fib	Variscan	Regional
Ser	Variscan? Eo-Alpine?	Regional
Ky	Eo-Alpine	Regional
St	Oligocene	Contact
Ms	Oligocene	Contact

Andalusite-bearing veins at Vedrette di Ries

Schists outcropping in the southern aureole of the Vedrette di Ries pluton contain several vein generations distinguished by their mineralogical composition. The following discussion considers only those veins which are discordant compared to the pervasive regional foliation, indicating that they



Figure 43 - Andalusite-quartz vein at Site 1. The vein is very thin and discontinuous.

are younger than (or contemporaneous with) Alpine deformation. Among these are some andalusite-bearing veins, which occur up to 1 km from the tonalite. The veins are thin, parallel-sided, filled fractures, generally straight and in parallel sets (Figure 43). They are oriented at a high angle to the

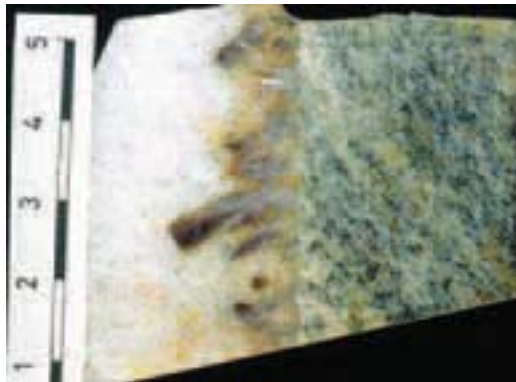


Figure 44 - Polished surface of an andalusite-quartz vein from Site 2, showing euhedral andalusite crystals which cluster at the straight vein wall; they exhibit concentric zoning with Fe-enriched darker areas. Base of photo: 5cm. From Cesare (1994b).

south-dipping foliation, and are not folded, implying that major ductile deformation did not affect the area during or after the vein formation.

The fine-grained pegmatitic structure and the euhedral shape of andalusite crystals (Figure 44) indicate crystallization within fluid-filled fissures.

Two sites with abundant veins in the area of Forcella Valfredda were chosen for further investigation (Figure 45). Site 1 is in the staurolite-andalusite zone, 800 m from the intrusion; Site 2, in the garnet-fibrolite

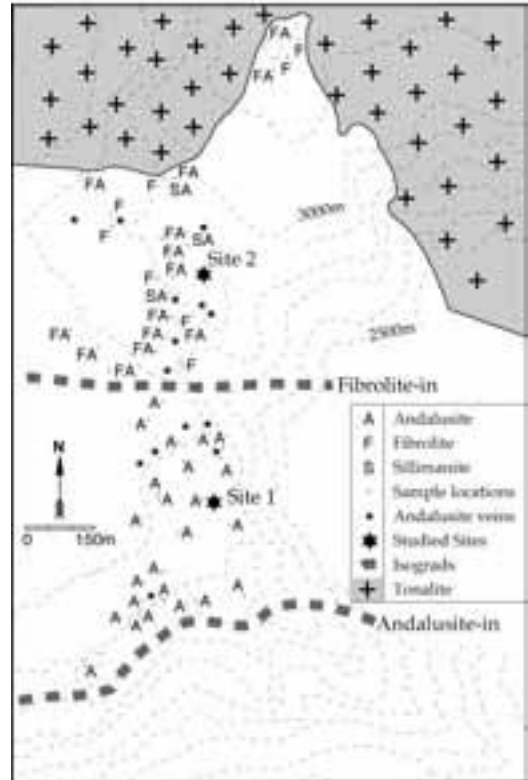


Figure 45 - Occurrences of andalusite-bearing veins and distribution of the Al_2SiO_5 polymorphs in the southern Vedrette di Ries aureole. After Cesare (1994b).

zone, is closer to the pluton. Figure 45 shows the distribution of the different Al_2SiO_5 polymorphs in the area, and the relationship between vein occurrence and andalusite presence within schists. Most of the vein occurrences reported in Figure 45 consist of single, thin veinlets. Therefore, the vein/host-rock volumetric ratio is extremely low.

At Site 1, host-rocks are pelitic hornfelses and schists containing quartz, plagioclase, andalusite, staurolite, biotite, ilmenite and graphite (\pm garnet \pm chlorite). They preserve the older penetrative planar foliation dipping south and a well-developed E-W subhorizontal stretching lineation.

Andalusite veins are very thin, usually < 1 cm and no longer than 1 metre. They contain quartz and andalusite in equal amounts, with variable biotite, and rare plagioclase and/or white mica. Biotite, which may reach up to 30%, is directly correlated to the abundance of garnet in the immediately adjacent host-rocks.

At Site 2, the country-rocks are pelitic hornfelses, composed of quartz, plagioclase, biotite, muscovite, acicular and prismatic sillimanite, garnet, ilmenite and graphite, with abundant relicts of andalusite.

Veins are larger and more abundant, and may in some cases reach a few metres in length and up to five cm in thickness.

Veins are discordant, their direction being quite random, but always very steep. There are two end-member types of andalusite-bearing pegmatitic veins at outcrop 2: biotite-absent, quartz-rich veins (the larger ones, Figure 44), and biotite-rich, quartz-poor veins. In the first type, euhedral andalusite crystals generally project from the vein walls into the quartz-rich inner zone as isolated prisms (up to 3 cm in length) or rosette aggregates. The second type occurs within garnet-bearing host-rocks; coarse-grained biotite is located at the vein walls, but also occurs in

the central portion of the veins, alone or associated with andalusite.

The veins show a mineralogical zoning with andalusite and biotite abundant at the vein borders, whereas quartz is dominant at the centre.

All of the andalusite-bearing veins occur within those parts of the aureole in which andalusite crystallized during contact metamorphism (cf. Figure 45), and are always hosted by andalusite-bearing rocks. Where veins occur in non-pelitic lithologies (e.g., pegmatitic gneiss or quartzite), they do not contain andalusite or biotite. In the few cases where veins crosscut different lithologies, there is a different mineral assemblage in each part. The general relationships between the mineralogy of veins and that of host-rocks are outlined in Figure 46.

The orientation of veins can be consistently related

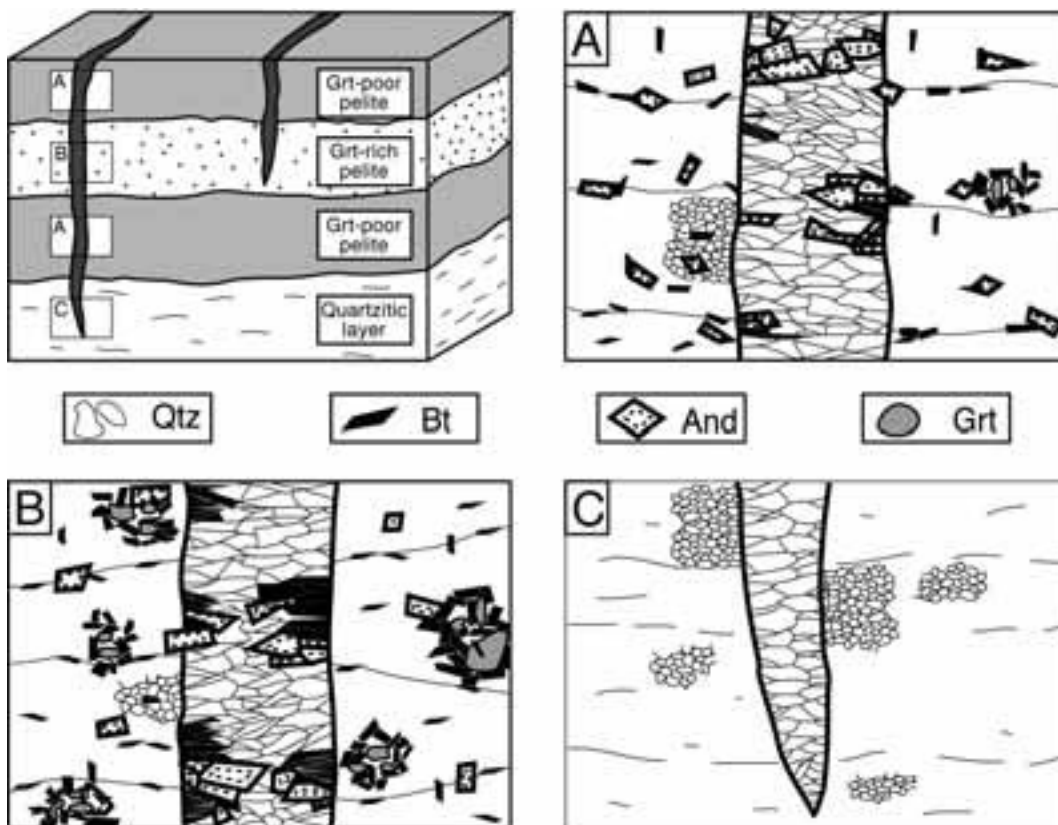


Figure 46 - Schematic diagram summarizing meso- and microstructural observations on the andalusite-bearing veins of the Vedrette di Ries aureole. Veins that formed in a layered rock (upper left) comprising metapelites and quartzite display a variable mineralogy, depending on the composition of the adjacent host-rock. A, B and C represent observed mineral composition and texture of veins in three end-member host-rock lithologies, respectively garnet-poor pelite, garnet-rich pelite, and quartzite. From Cesare (1994b).

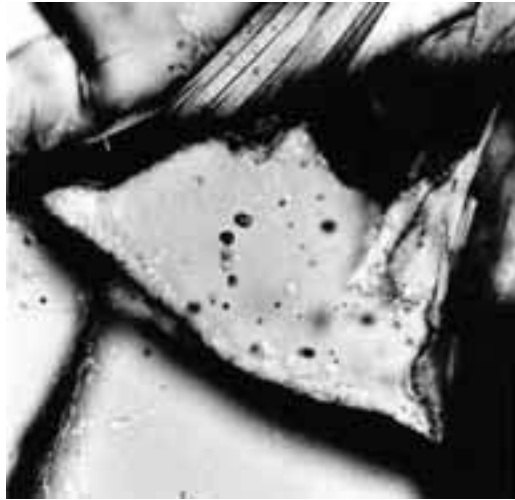


Figure 47 - Primary fluid inclusions in quartz crystals from within Andalusite-bearing veins.

to the stress field generated by the emplacement of the underlying tonalite, which gives a subvertical σ_1 . In particular, the N-S vein directions at outcrop 1 are concordant with the marked elongation of the pluton, which defines the E-W direction of minimum principal stress in the schists.

The fluid inclusions within quartz of Andalusite-bearing veins (Figure 47) have been studied by Cesare and Hollister (1995).

Their results suggest that the fluids present during vein formation are those occurring in the isolated fluid inclusions defined as Type A. These are water-rich $H_2O-CO_2-CH_4-NaCl$ mixtures, with low salinity and high CO_2/CH_4 ratio. The composition and density of these "primary" inclusions are consistent with a C-O-H fluid in equilibrium with graphite at the estimated P-T conditions of veining, and with a regime of lithostatic fluid pressure during crystallization of vein minerals. The low salinity of the aqueous fraction indicates that increased solubility in 'aggressive' fluids (e.g. Kerrick, 1990) is not required for effective aluminum transport. In the inclusions, density changes are variously recorded in each sample as a function of the degree of strain and of the relative abundance of quartz and andalusite.

Based on field, microstructural and fluid inclusion data, a mechanism of synmetamorphic veining (Cesare, 1994b; Cesare et al., 2001) is here summarized. It accounts for the processes of fracture opening, migration of matter, and precipitation of

minerals during the formation of the Andalusite-bearing veins.

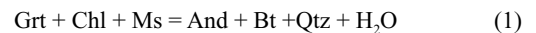
Vein Opening: Timing, Mechanisms, and Fluid Behaviour

Veins formed during the contact metamorphic event, before the crystallization of sillimanite. At that time the P-T conditions were within the stability field of andalusite ($T = 500 \pm 50$ °C, Cesare, 1992), and schists were undergoing further heating. Furthermore, growth of andalusite in veins and host-rocks was coeval. Hence, mineral precipitation in veins was synmetamorphic: it was synchronous with metamorphic reactions taking place in the host-rock at the time of vein formation.

Hydraulic extension fracturing (hydrofracturing) requires elevated fluid pressures and low deviatoric stress, and generates fractures perpendicular to σ_3 . It occurs when the fluid pressure (P_f), exceeds the sum of minimum stress (σ_3) and tensile strength of the rock (σ_0), according to the failure condition:

$$P_f \geq \sigma_3 + \sigma_0$$

In the example studied, the hydrofracturing model is consistent with the orientation of veins compared to the stress field induced by the underlying tonalite. Since the typical features of shear fracturing are minimal, it can be concluded that the main mechanism of vein opening was hydrofracturing, caused by fluid release during devolatilization reactions. Decrease in modal chlorite and white mica, which is recorded proceeding upgrade within the andalusite zone of the aureole, is clear evidence that host-rock metapelites were undergoing dehydration during andalusite formation. Combining the above data with the textural observation of biotite pseudomorphing garnet, the reaction



can be proposed as one plausible dehydration reaction in the hornfels capable of producing the vein mineral assemblage.

Opening of fissures in the rock generates a sudden increase in the volume available for the fluid phase, and a consequent drop in pore pressure. Fractures become a source for local pressure gradients which immediately drive fluids into the open cavities, filling them. However, to keep a vein open, fluid pressure in the vein must be equal to σ_3 : after a rapid initial fluid flow toward the cavity, a condition of mechanical stability between fracture and host-rock will be attained and will inhibit pressure gradients and permanent flow. Frequent occurrences of isolated, thin, andalusite-bearing veins in the studied aureole, and the lack of interconnected vein networks are

additional observations against large-scale fluid circulation.

Mass transfer and mineral deposition

After the initial, transient flow, fluid can be considered as virtually stagnant, acting as a passive medium, in thermal and mechanical equilibrium with the surrounding rocks. Moreover, chemical equilibrium can also be assumed, given present theoretical models and the equal parageneses and mineral chemistry in vein and host-rock. It follows that crystallization of vein minerals was simply controlled by heterogeneous mineral reactions in the host-rock (e.g. reaction 1).

Nucleation of product phases (andalusite, biotite and quartz) is favoured on the strained minerals at vein walls; once nuclei form, concentration and chemical potential gradients between reactants and products are established, and the transfer of chemical components, continuously provided by dissolving reactants, is activated. This implies synchronous growth of andalusite in vein and host-rock. Mass transfer from adjacent host-rock to the vein occurs via intercrystalline diffusion, which can be very effective, and dominant during metamorphism. Since the fracture is filled with fluid that allows for faster diffusion, the growth of vein minerals is also faster and grain-size coarser; this explains the pegmatitic vein texture.

Because intergranular diffusion is the mass-transfer process during synmetamorphic veining, diffusion halos around veins can be expected. The plagioclase-rich border zones that sometimes occur at vein margins can be interpreted as diffusion halos. Conversely, such an explanation is not applicable to the biotite-rich zones, which are located within the veins, and cannot be interpreted as residual portions of metasomatically-depleted country rocks.

DAY 4

Anterselva (Antholz) valley - Passo Stalle (Staller Sattel) - Brunico (Bruneck).

Morning: descent to Anterselva. Outcrops of tonalite at Cima di Vila (Zinsnock): discussion of its geochemical and petrologic features (Bellieni, 1980; Bellieni et al. 1982) and of the genetic relationships with the Vedrette di Ries Pluton.

Afternoon: Drive to Passo Stalle (Staller Sattel) (2000 m asl): cross sections along the cataclases and mylonites of the Defereggen-Anterselva-Valles (DAV) line from the pass to the Vedrette di Ries tonalite. Shear bands in greenschist facies rocks, indicating the sinistral kinematics of the DAV. High-

and low-temperature deformation of the tonalite, and its relationships to the DAV mylonites. In this area the southern contact of the pluton dips steeply to the south, concordantly to the mylonites of the DAV. No kinematic indicators have been found within the tonalite, but preserved magmatic foliations parallel to the mylonitic foliation of the DAV call for syntectonic intrusion. This part of the pluton is inferred to be the feeder of the main body located further to the north. This conclusion is based on the occurrence of a steep magmatic foliation associated with steep lineations (Steenken et al., 2000; Wagner et al., in review). The location of the feeders of the intrusive bodies along segments of the Periadriatic Lineament is a common feature of the Periadriatic plutons.

Discussion of the emplacement mechanisms within the framework of the Oligocene tectonics of the Eastern Alps.

DAY 5

Return to Florence - End of Field Trip.

Acknowledgments

Financial support was received from CARG-PAB, the Province of Bolzano, from CNR-IGG, from the University of Padova and from DFG (Project Ha 2403/3-2). We wish to thank Gottfried Leitgeb (Rif. Forcella Valfredda), Arnold Seeber (Rif. Roma) and Maria Mair (Geltalalm) for their assistance during field work. The critical reading of Giuliano Bellieni is gratefully acknowledged.

References

- Bassani S., Fioretti A.M., Bellieni G. (1997). Il granato nelle masse intrusive di Rensen, Vedrette di Ries e Polland (Alpi Orientali). *Plinius n.18*; 43-44.
- Bellieni G. (1977). Caratteri geobarometrici delle intrusioni granitiche del plutone delle Vedrette di Ries (Rieserferner)(Alto Adige Orientale) alla luce dei sistemi sperimentali Q-Or-Ab-An-H₂O. *Rend. Soc. It. Miner. Petr.*, 33, 631-645.
- Bellieni G. (1978) Caratteri geochimici del massiccio granodioritico-tonalitico delle Vedrette di Ries (Rieserferner)-Alto Adige Orientale. *Rend. Soc. It. Miner. Petr.*, 34, 527-548.
- Bellieni G. (1980) The Cima di Vila (Zinsnock) Massif: Geochemical features and comparisons with the Vedrette di Ries (Rieserferner) pluton (Eastern Alps-Italy). *Neu. Jb. Mineral. Abh.*,

- 138, 244-258.
- Bellieni G., Comin Chiaramonti P., Visonà D. (1976). Contributo alla conoscenza del plutone delle Vedrette di Ries (Alpi Orientali). *Boll. Soc. Geol. It.*, 95, 351-370.
- Bellieni G., Molin G.M., Visonà D. (1979) The petrogenetic significance of the garnets in the intrusive massifs of Bressanone and Vedrette di Ries (Eastern Alps-Italy). *Neu. Jb. Mineral. Abh.*, 136, 238-253.
- Bellieni G., Peccerillo A., Poli G. (1981). The Vedrette di Ries (Rieserferner) Plutonic Complex: Petrological and Geochemical Data Bearing on Its Genesis. *Contrib. Mineral. Petrol.*, 78, 145-156.
- Bellieni G., Peccerillo A., Poli G. (1982) REE distribution in the Cima di Vila (Zinsnock) granodioritic complex and its petrogenetic significance (Eastern Alps, Italy). *Neu. Jb. Mineral. Abh.*, 145, 50-65.
- Bellieni G., Cavazzini G., Fioretti A.M., Peccerillo A., Poli G., Zantedeschi P. (1989). Petrology and geochemistry of microgranular mafic enclaves from the Vedrette di Ries plutonic complex (Eastern Alps). *Per. Mineral.*, 58, 1-3, 45-65.
- Bellieni G., Justin Visentin E., Zanettin B. (1995). Use of the chemical TAS diagram (Totali Alkali Silica) for classification of plutonic rocks: problems and suggestions. *Soc. It. Mineral. Petrol. Plinius*, 14, 49-52.
- Bianchi A. (1934). Studi petrografici sull'Alto Adige orientale e regioni limitrofe. *Mem. Ist. Geol. R. Univ. Padova*, 10, 243pp.
- Bigi, G., A. Castellarin, M. Coli, G. V. Dal Piaz, M. Sartori, P. Scandone, and G. B. Vai (1990) Structural model of Italy, S.E.L.C.A., Florence (Italy).
- Borsi S., Del Moro A., Sassi F.P., Zanferrari A., Zirpoli G. (1978). New geopetrologic and radiometric data on the alpine history of the austridic continental margin South of the Tauern Window (Eastern Alps). *Mem. Sci. Geol.*, 32, 17pp.
- Borsi S., Del Moro A., Sassi F.P., Zirpoli G. (1973). Metamorphic evolution of the Austridic rocks to the south of the Tauern Window (Eastern Alps): radiometric and geopetrologic data. *Mem. Soc. Geol. It.*, 12, 549-571.
- Borsi S., Del Moro A., Sassi F.P., Zirpoli G. (1979). On the age of the Vedrette di Ries (Rieserferner) massif and its geodynamic significance. *Geol. Rdsch.*, 68, 41-60.
- Cesare B. (1992). Metamorfismo di contatto di rocce pelitiche nell'aureola di Vedrette di Ries (Alpi Orientali, Italia). *Unp. PhD Thesis, Univ. Padova*, 106 pp.
- Cesare B. (1994a). Hercynite as the product of staurolite decomposition in the contact aureole of Vedrette di Ries, eastern Alps, Italy. *Contributions to Mineralogy and Petrology*, 116, 239-246.
- Cesare B. (1994b). Synmetamorphic veining: origin of andalusite-bearing veins in the Vedrette di Ries contact aureole, Eastern Alps, Italy. *Journal of Metamorphic Geology*, 12, 643-653.
- Cesare B. (1999). Multi-Stage pseudomorphic replacement of garnet during polymetamorphism: Microstructures and their interpretation. *Journal of Metamorphic Geology*, 17, 723-734
- Cesare B. (1999). Multi-Stage pseudomorphic replacement of garnet during polymetamorphism: 2. algebraic analysis of mineral assemblages. *Journal of Metamorphic Geology*, 17, 735-746
- Cesare B. and Hollister L.S. (1995). Andalusite-bearing veins at Vedrette di Ries (Eastern Alps - Italy): fluid phase composition based on fluid inclusions. *Journal of Metamorphic Geology*, 13, 687-700.
- Cesare B., Poletti E., Boiron M-C. & Cathelineau M. (2001). Alpine metamorphism and veining in the Zentralgneis Complex of the SW Tauern Window: a model of fluid-rock interactions based on fluid inclusions. *Tectonophysics*, 336, 121-136
- Cescutti C., Fioretti A.M., Bellieni G. & Cesare B. (2003). Studio petrografico e geochimico dei filoni porfirici acidi affioranti nel basamento austroalpino nei dintorni di Vedrette di Ries (Alto Adige Orientale). *GeoItalia 2003 Congress, Abstract* pg. 201
- Chopin, C., Henry, C., and Michard, A. (1991) Geology and petrology of the coesite-bearing terrain, Dora-Maira Massif, western Alps. *Eur. J. Mineral.*, 3, 263-291.
- Dal Piaz, Gb., (1934). Studi geologici sull'Alto Adige orientale e regioni limitrofe. *Memorie Istituto di Geologia Regia Università di Padova*, 10, 242 pp.
- Dal Piaz G.V., Von Raumer J., Sassi F.P., Zanettin B., Zanferrari A. (1975). Geological outline of the Italian Alps. Reprinted from "Geology of Italy" Coy Squyres Ed. The Earth Sciences Society of

- the Libyan Arab Republic. Tripoli.
- Dal Piaz G.V., Venturelli G., 1983. Brevi riflessioni sul magmatismo post-ofiolitico nel quadro dell'evoluzione spazio-temporale delle Alpi. *Memorie Società Geologica Italiana*, 26, 5-19.
- Exner C.H., (1976). Die Geologische Position der Magmatite des periadriatischen Lineaments. *Verh. Geol.*, B 4:3-64.
- Froitzheim, N., Schmid, S.M., and Fey, M. (1996) Mesozoic paleogeography and the timing of eclogite-facies metamorphism in the Alps: A working hypothesis. *Eclogae geol. Helv.*, 89, 81-110.
- Gatto G.O., Gregnanin A., Molin G.M., Piccirillo E.M., and Scolari A. (1976). Le manifestazioni Andesitiche polifasiche dell'Alto Adige occidentale nel quadro geodinamico alpino. *St. Trentin. Sc. Nat.*, 53, 21-47.
- Guidotti C.V., (1968). Prograde muscovite pseudomorphs after staurolite in the Rangeley-Oquossoc areas, Maine. *American Mineralogist*, 53, 1368-1376.
- Green T.H. (1972). Crystallization of calc-alkaline andesite under controlled high-pressure hydrous conditions. *Contrib. Mineral. Petrol.* 34, 150-166.
- Green T.H., and Ringwood A.E. (1972). Crystallization of garnet-bearing rhyodacite under high-pressure hydrous conditions. *J. Geol. Soc. Aust.* 19, 203-212.
- Hammerschmidt K. (1981). Isotopengeologische Untersuchungen am Augengneis vom Typ Campo Tures bei Rain in Taufers, Südtirol. *Mem. Sci. Geol.*, 34, 273-300.
- Hofmann K.H., Kleinschrodt R., Lippert R., Mager D. und Stöckert B. (1983). Geologische Karte des Altkristallin südlich des Tauernfensters zwischen Pfunderer Tal und Tauferer Tal (Südtirol). *Der Schlern*, 57; 572-590.
- Holdaway M.J. (1971). Stability of andalusite and the aluminum silicate phase diagram: *American Journal of Science*, 271, 97-131
- Kagami H., Ulmer P., Hansmann W., Dietrich V., and Steiger R.H. (1991). Nd-Sr isotopic and geochemical characteristics of the Southern Adamello (northern Italy) intrusives: implication for crustal versus mantle origin. *J. Geophys. Res.* 96, 14331-14346.
- Kerrick D.M. (1990). The Al₂SiO₅ polymorphs. *Reviews in Mineralogy*, 22.
- Kleinschrodt R. (1987). Quarzkorngefügeanalyse im Altkristallin südlich des westlichen Tauernfensters (Südtirol/Italien). *Erlanger Geol. Abh.*, 114, 1-82.
- Kozur, H. (1991) The evolution of the Meliata-Halstatt ocean and its significance for the early evolution of the Eastern Alps and Western Carpathians. *Paleogeogr. Paleoclimatol. Paleoecol.* 87, 109-135.
- Laubscher H.P. (1985). The late Alpine (Periadriatic) intrusions and the Insubric Line. *Mem. Soc. Geol. It.*, 26, 21-30.
- Mager D. (1985). Geologische Karte des Rieserfernergruppe zwischen Magerstein und Windschar (Südtirol). *Der Schlern*, 6, Bozen
- Mancktelow N.S., Stöckli D.F., Grollimund B., Müller W., Fügenschuh B., Viola G., Seward D. and Villa I.M. (2001). The DAV and Periadriatic fault systems in the eastern Alps south of the tauern Window. *Int. J. Earth Sci.*, 90, 593-622.
- Mann A. and Scheuven D. (1998). Structural investigation of the northern contact of the Rieserferner Plutonic Complex (Eastern Alps) - first results. *Terra Nostra*, 98, 62.
- Müller W., Mancktelow N.S. and Meier M. (2000). Rb-Sr microchrons of synkinematic mica in mylonites: an example from the DAV fault of the Eastern Alps. *Earth and Planetary Science Letters*, 180, 385-397
- Müller W., Prosser G., Mancktelow N.S., Villa I.M., Kelley S.P., Viola G., and Oberli F. (2001). Geochronological constraints on the evolution of the Periadriatic fault system (Alps). *Int. J. Earth Sci.*, 90, 623-653.
- Neubauer, F. (1994) Kontinentkollision in den Ostalpen. *Geowissenschaften* 12, 136-140.
- Pattison, D.R.M. & Tracy, R.J., 1991: Phase equilibria and thermobarometry of metapelites. In: Kerrick, D.M. (ed.): *Contact metamorphism*. Reviews in Mineralogy, 26; 43-104
- Prochaska W. (1981). Einige Ganggesteine der Rieserfernerintrusion mit neuen radiometrischen Altersdaten. *Mitteilungen der Gesellschaft der geologie und Berbaustudent, Wien*, 27, 161-171.
- Rosenberg, C.L., A. Berger, and S. M. Schmid (1995) Observations from the floor of a granitoid pluton; inferences on the driving force of final emplacement, *Geology*, 23, 443-446.
- Rosenberg, C. L., in press, Shear zones and magma ascent: A model based on a review of the Tertiary magmatism in the Alps. *Tectonics*.
- Sassi, F.P. & Zanettin, B. (1980) Schema degli eventi

- metamorfici e magmatici nelle Alpi Orientali. *Rendiconti Società Italiana di Mineralogia e Petrologia*, 36; 3-7.
- Santilli M., Orombelli G. and Pelfini M. (2002). Variations of Italian glaciers between 1980 and 1999 inferred by the data supplied by the Italian Glaciological Committee. *Geogr. Fis. Dinam. Quat.* 25, 61-76.
- Schulz B. (1989). Jungalpidische Gefügeentwicklung entlang der Deferegggen-Antholz-Vals-Linie (Osttirol, Österreich). *Jahrbuch. Geol. Bundesanst.*, 132; 775-789.
- Schulz B. (1997). Pre-Alpine tectonometamorphic evolution in the Austroalpine basement to the south of the central Tauern Window. *Schweizerische Mineralogische Petrographische Mitteilungen*, 77, 281-297.
- Steenken A., Siegesmund, S. and Heinrichs, T. (2000). The emplacement of the Rieserferner Pluton: Constraints from field observations, magnetic fabrics and microstructures. *Journal of Structural Geology*, 22, 1855-1873
- Steenken A. (2002). The emplacement of the Rieserferner Pluton and its relation to the DAV-Line as well as to the kinematic and thermal history of the Austroalpine basement (Eastern Alps, Tyrol) *Geotektonische Forschungen*, 94, 120 pp.
- Steenken A, Siegesmund S, Heinrichs T, Fugenschuh B (2002). Cooling and exhumation of the Rieserferner Pluton (Eastern Alps, Italy/Austria). *Int. J. Earth Sci.*, 91, 799-817.
- Stöckhert B. (1984). K-Ar determinations on muscovites and phengites from deformed pegmatites, and the minimum age of the Old Alpine deformation in the Austridic basement to the south of the western Tauern Window (Ahrn valley, Southern Tyrol, Eastern Alps). *Neu. Jb. Mineral. Abh.*, 150, 103-120.
- Stöckhert B. (1985). Pre-Alpine history of the Austridic basement to the south of the western Tauern Window (Southern Tyrol, Italy). Caledonian versus Hercynian event. *Neu. Jb. Geol. Paläont. Mh.*, 618-642.
- Stöckhert B. (1987). Das Uttenheimer Pegmatit-Feld (Ostalpinen Altkristallin, Südtirol) Genese und alpine Überprägung. *Erlanger Geol. Abh.*, 114, 83-106.
- Trommsdorff V. and Nievergelt P., (1983) The Bregaglia (Bergell) Iorio Intrusive and its field relations. *Mem. Soc. Geol. It.*, 26, 55-68.
- Von Blankenburg F. and Davis J.H. (1995). Slab breakoff: A model for syncollisional magmatism and tectonics in the Alps. *Tectonics* 14, 120-131.
- Wagner R., C. L. Rosenberg, M.R. Handy, C. (2003). *Memorie di Scienze Geologiche (Padova)*, 54,
- Wagner R., C. Rosenberg L., Handy M.R., Möbus C., and Albertz M. in review, Buoyancy-driven inflation of a mid-crustal sill fed by a transpressive shear zone: The Rieserferner Pluton, Eastern Alps. *Geol. Soc. Am. Bull.*

Back Cover:
*Road map of the area NE of Brunico.
Numbers in yellow dots indicate the localities
of each field trip's day as in the Guide.*

FIELD TRIP MAP

32nd INTERNATIONAL GEOLOGICAL CONGRESS



Edited by APAT